Effect on Pavement Wear of Increased Mass Limits for Heavy Vehicles – Concluding Report

G. Arnold, B. Steven, D. Alabaster & A. Fussell

Land Transport New Zealand Research Report 281

ISBN 0-478-25392-3
ISSN 1177-0600

PO Box 2840, Waterloo Quay, Wellington, New Zealand
Telephone 64 4 931 8700; Facsimile 64 4 931 8701
Email: *research@landtransport.govt.nz*
Website: *www.landtransport.govt.nz*

Arnold, G.,[1] Steven, B.,[2] Alabaster, D.,[3] Fussell, A.[3] 2005. Effect on pavement wear of increased mass limits for heavy vehicles – concluding report. *Land Transport New Zealand Research Report 281.* 80pp.

[1] Formerly PaveSpec Ltd, 30 Balfour St, Mornington, Wellington, now Transit New Zealand, PO Box 5084, Lambton Quay, Wellington
[2] University of Canterbury, Private Bag 4800, Christchurch, New Zealand
[3] Transit New Zealand, PO Box 1479, Christchurch

Keywords: accelerated pavement testing, CAPTIF, heavy vehicles, loads, loading, mass limits, New Zealand, pavement, pavement loading, pavement performance, pavement wear, roads, road user charges, surface texture, thin-surfaced pavements, traffic, vehicles

An important note for the reader

This report is the final stage of a project commissioned by Transfund New Zealand before 2004, and is published by Land Transport New Zealand.

Land Transport New Zealand is a Crown entity established under the Land Transport New Zealand Amendment Act 2004. The objective of Land Transport New Zealand is to allocate resources in a way that contributes to an integrated, safe, responsive and sustainable land transport system. Each year, Land Transport New Zealand invests a portion of its funds on research that contributes to this objective.

While this report is believed to be correct at the time of its preparation, Land Transport New Zealand, and its employees and agents involved in its preparation and publication, cannot accept any liability for its contents or for any consequences arising from its use. People using the contents of the document, whether directly or indirectly, should apply and rely on their own skill and judgement. They should not rely on its contents in isolation from other sources of advice and information. If necessary, they should seek appropriate legal or other expert advice in relation to their own circumstances, and to the use of this report.

The material contained in this report is the output of research and should not be construed in any way as policy adopted by Land Transport New Zealand but may be used in the formulation of future policy.

Contents

List of Figures

List of Tables

Executive summary

Introduction

The road transport industry in New Zealand has been lobbying for increases in the allowable mass limits for heavy vehicles on the basis that this would give increased efficiency and benefits to the economy. Some of the proposals for increased mass limits involve increased axle load limits which would clearly lead to additional pavement wear. Road controlling authorities, while sharing the industry's aims for increased efficiencies in the road transport system, are concerned that any additional pavement wear generated by higher axle loads will be paid for, so that the standard of the roading network can be maintained.

At present (2005) Road User Charges (RUCs) are based on the fourth power law, which was developed from the AASHO road test in the United States in the 1950s. The pavements and vehicles used for that test differ considerably from those in use in New Zealand today.

In response to possibly inevitable increases in mass limits of heavy vehicles on New Zealand roads, a four-year research study (between 2001 and 2004) at the Canterbury Accelerated Pavement Testing Indoor Facility (CAPTIF, Christchurch, New Zealand), was undertaken.

Accelerated Pavement Tests

This report represents the analysis of results of the study. The aim of the testing was to compare the effect of mass (of 8, 10 and 12 tonne single axle dual tyres) on pavement wear for a range of pavements which are more typical of those used on New Zealand roads.

Two major accelerated pavement tests for 1,000,000 passes were used to monitor pavement wear as indicated by rutting. After 1,000,000 passes had been applied, the loads were increased from 8 tonnes to either 10 or 12 tonnes, and a further 300,000 to 400,000 cycles were applied.

The CAPTIF pavements were all surfaced with 25 mm of asphaltic concrete. Two additional tests were conducted on chipseal-surfaced pavements to compare the rate of surface texture depth deterioration between 8 and 10 tonne axles and 8 and 12 tonne axles.

Analysis

To analyse the two major accelerated pavement tests, vertical surface deformation (VSD) was used as the main measure of pavement wear. VSD is directly related to rutting, and longitudinal variability in VSD leads to increased roughness. The VSD measurements were extrapolated to determine the number of wheel passes needed to reach a VSD of 15 mm, which was used to define pavement end-of-life. The end-of-life for the pavement segments for both the heavy (10 or 12 tonne, P_L) and light wheelpaths (8 tonne, P_{8t}) was

determined when 10% of the pavement segment equalled or exceeded the end-of-life criterion of 15 mm). From the pavement lives for the two wheelpaths (N_L and N_{8t}) the damage law exponent n was determined using the following equation:

$$n = \frac{log\left(\frac{N_{8t}}{N_L}\right)}{log\left(\frac{P_L}{P_{8t}}\right)}$$

The damage law exponent n is used to calculate the traffic loading in terms of Equivalent Standard Axles (ESAs) for pavement design and deterioration modelling. It is also used in determining the level of RUCs where a current value of 4 is assumed, hence the name fourth power law. Therefore, determining the damage law exponent value for the results has the advantage that it can be used directly in current methods of pavement design and deterioration modelling.

Changes in texture depth were monitored in the two chipseal tests and the Patrick log model used for chipseal design was fitted to the data. The Patrick model relates traffic in terms of equivalent light vehicles (elv) to changes in texture depth as is done in chipseal design. Assuming the 8-tonne axle was equivalent to 10 passes of light vehicles, the number of elvs for the 10-tonne and 12-tonne axles were determined. This relative difference in chipseal deterioration was also compared in terms of a damage law. A damage law can be used for determining the design traffic, which includes a range of heavy vehicles in the traffic spectra which will not be affected by any increases in mass limits.

Conclusions

RUCs are governed by pressures other than road and pavement deterioration and are therefore not discussed in detail in this report. In general however, the results of this study in terms of assigning the appropriate damage law exponent for pavement design would also be appropriate for calculating RUCs.

General

- VSD, which is a fundamental form of pavement wear that results in both rutting and increased surface roughness, again proved to be the most useful measure for monitoring pavement wear at CAPTIF.
- The end-of-life for the pavement segment was defined as the number of wheel passes when 10% of the area has a VSD greater or equal to 15 mm.
- Only a small range of pavements was tested at CAPTIF. The subgrade used at CAPTIF for all pavement test segments was a silty clay with a CBR of 11%, while the aggregate types were different, and the pavement thickness was either 300 mm or 250 mm.
- The damage law exponent which relates the relative lives of axle loadings to a standard load, is a key parameter used in calculating RUCs. It is also used to determine the design traffic loading in terms of ESAs for pavement design and deterioration modelling. Therefore assessing the impact of increases in mass limits by way of determining the appropriate damage law exponent has the advantage of

being able to input the results of this research directly into calculating RUCs, pavement design, and deterioration modelling.

Pavement life

- Pavement life, in terms of the number of wheel passes until the VSD was equal to 15 mm, was best estimated by a best fit linear projection to the data from 150,000 to 1 000,000 cycles (after the initial compaction period).
- This linear projection is effectively the compaction–wear model proposed in previous reports for the mass limits study (VSD = Comp. + N . Wear).
- An extrapolation power model was also fitted to the data to determine the pavement life, but its use was rejected because it predicts unrealistic pavement lives. Further, the World Bank HDM-III deterioration models assume a linear model for rut depth and thus the linear projection was adopted.
- The end-of-life for a pavement segment was defined as the number of wheel passes when 10% of the area had a VSD greater or equal to 15 mm. This was calculated as the 10^{th} percentile value of lives for each individual station in each segment and wheelpath.
- With the exception of three segments, nearly all pavements had lives between 2,400,000 and 2,800,000 passes of the 40 kN dual-tyred wheel load (equivalent to the current legal load of a single dual-tyred axle of 8.2 tonnes).
- The pavement segment constructed from rounded aggregates had the shortest life with 10% reaching 15 mm VSD in 400,000 passes of a 40 kN dual-tyred wheel load. Actual stations failed completely at 250,000 passes.
- Results from the first Australian basecourse pavement segment that required many surface repairs were omitted because the repairs reduced the measured VSD.
- The pavement segment constructed with recycled crushed concrete was the best performer, as it achieved a predicted pavement life of 4,300,000 passes of a 40 kN dual-tyred wheel load. This is almost twice the life achieved with the other pavements of the same depth.

Pavement damage law exponents, n

- Based on the pavement segment lives predicted in the heavy (50 or 60 kN) and light (40 kN) wheelpaths, the calculated damage law exponents ranged from 1.1 to 3.4.
- The lowest damage law exponent of 1.1 was calculated for the pavement segment constructed with recycled crushed concrete.
- A damage law exponent of 3.2 was calculated for the pavement constructed with rounded aggregate which had the shortest life. This suggests that the damage law exponent is related to pavement strength.

Subgrade strain

The use of back-calculated vertical compressive strain on the top of the subgrade, as used in pavement design to predict life, was tested on the results of the CAPTIF pavement segments. Results were:

- For CAPTIF segments with nearly the same pavement life (approx. 1,200,000 passes of a 12-tonne dual-tyred axle), the subgrade strain calculated ranged from 1500 to 2500 micro-strain. This equates to a range of lives predicted with the Austroads subgrade strain criterion of between 6,000 and 240,000 cycles.
- The Austroads subgrade strain criterion grossly underpredicts the pavement life by between 5 and 200 times less than the actual life.
- Subgrade strain varied significantly and bore no relationship to pavement life.

Pavement Structural Number (SNP)

SNP is a single parameter that classifies pavement strength and has been widely used in deterioration modelling and in pavement design. Two methods of calculating the SNP, as recommended by Transit New Zealand, were investigated for relationships between pavement life and/or damage law exponent. Results of this analysis were as follows:

- Relationships between SNP and pavement life are best when using the 10^{th} percentile value of SNP and, unless otherwise mentioned, this is the value that is used in this report.
- Relationships between SNP and pavement life are best in the heavier (50 kN and 60 kN) wheelpaths.
- The pavement segment constructed with rounded aggregate had the shortest life but was not identified as having a low SNP calculated from pavement layer moduli. However the lowest SNP was calculated for this segment using the FWD measurements directly in the 'SNP from FWD' equation.
- Excluding the above segment's results, the 'SNP value from moduli' compared with SNP from FWD showed the best relationships with pavement life (R^2= 0.65 in the heavier wheelpath and R^2=0.36 in the lighter wheelpath).
- Good relationships between 'SNP from moduli' and damage law exponent were obtained if the results for the much repaired segment with the first Australian basecourse were omitted.
- Good relationships between 'SNP from FWD' and damage law exponent were obtained if the results for the repaired and the recycled segments were omitted.
- The relationship with SNP determined from pavement layer moduli is best to use for the design of new pavements, while the relationship from FWD measurements is best used when interpreting FWD measurements on existing pavements.
- Reasonable relationships using the damage law exponent could only be determined from FWD measurements made in the heavy wheelpath after at least 30,000 wheel passes. This suggests that FWD surveys carried out before the introduction of any increase in mass limits may not identify areas of pavement weaknesses where a high damage law exponent is considered the most appropriate.

Initial deformation

- Without exception for all new pavements, a significant amount of deformation occurs in the first 150,000 cycles.
- This initial deformation can be predicted adequately using the HDM-III method for calculating the secondary compaction rut depth because the damage law exponent for the compaction portion is the same as that determined from the pavement lives. Therefore the ESAs calculated in the formula for rut depth caused by secondary compaction are correct.
- With the exception of three pavement segments, increasing load on the wheelpath previously trafficked with 1,000,000 passes of the 40 kN wheel load resulted in additional secondary compaction similar in magnitude to that which occurred on the newly constructed pavement for the same load.
- Two of the three pavements that did not suffer secondary compaction caused by an increase in load on an already trafficked pavement, had been constructed with the Australian aggregate from Montrose, Victoria.
- The other pavement that did not undergo secondary compaction because of an increase in load on an already trafficked pavement, had been constructed using New Zealand AP40 aggregate complying with TNZ M/4 but contaminated with 10% by mass of silty clay fines.

Pavement modelling

The range of CAPTIF pavements studied was limited in size. Therefore to determine if trends in results could be applied to other pavement depths and subgrade strengths, additional pavements were modelled. Results from this pavement modelling follow.

- The predicted VSD from the pavement model was slightly higher than the measured values for the CAPTIF pavement used for validation.
- The relative differences between the 40 kN and 60 kN wear, and the damage law exponents that are computed with the model were the same as the actual damage law exponent determined for the test pavement.
- The model was expanded to predict the damage law exponent for thick (700 mm) and thin (300 mm) pavements over strong (CBR=10%) and weak (CBR=5%) subgrades.
- The damage law exponent values computed from the pavement models supports the trends determined from the measured data. The poorer fit with the SNP determined from FWD measurements is most likely related to the inaccurate prediction of FWD deflections from the finite element program DEFPAV.
- The pavement model presented in this report represents a more fundamental method of design in terms of predicting the pavement rut depth. It can provide a method to predict the pavement life of pavements constructed with materials that do not comply with existing specifications (e.g. recycled materials). It also has application in determining damage law exponents for a range of other loads and tyre types.

Chipseal surfacing

Two tests on chipseal surfacings were conducted for 8- versus 10-tonne and 8- versus 12-tonne loads. Conclusions are as follows:

- An increase in mass limits is likely to reduce the life of chipseal surfacings on New Zealand roads. This reduction has occurred on a private forestry road used by vehicles with axle loads nearly double the current New Zealand legal limit.
- The Patrick model, which forms the current basis of chipseal performance prediction, relates texture depth with the number of passes of light vehicles. It also fits well the mid-range of the measured mean profile depth (i.e. it gives results that are similar to texture depth) with load cycles.
- The assumption is that an 8-tonne standard axle is equivalent to 10 passes of light vehicles (in chipseal design, one pass of an HCV is assumed as equivalent to 10 passes of light vehicles). Then from the 8- versus 10-tonne test, the 10-tonne axle is equivalent to 18 passes of light vehicles, while for the 8- versus 12-tonne test, the 12-tonne axle was equivalent to 29 passes of light vehicles.
- Relative damage in terms of deterioration of chipseal texture depth was compared using the damage law exponent method. For the 8- versus 10-tonne test, a damage law exponent of 3.1 was calculated, while a value of 2.0 was calculated in the 8- versus 12-tonne test. Combining both datasets resulted in an exponent of 2.7.
- When calculating chipseal design traffic loadings in terms of number of light vehicles, ESAs should replace HCV, so that 1 ESA is equal to 10 light vehicle passes. This allows for an uptake by only some HCVs of any increases in mass limits if required.

Road User Charges (RUC)

- The most appropriate damage law exponent for use in RUCs should be the same value as determined from the SNP used for pavement design.
- If mass limits are increased, the damage law exponent value may be reduced from the current value of 4 for specific routes which have relatively high strength pavements. This reduction could be incorporated when assigning RUCs for vehicles which can employ the increase in mass limits.
- Conversely, damage law exponents for low-strength low-volume roads could increase.

Recommendations

Key recommendations that arise from this study are:

- When calculating traffic loading for design and deterioration modelling then the appropriate damage law exponent in relation to the SNP should be used.
- The use of SNP is recommended to predict pavement life rather than use the subgrade strain.

- As a conservative approach, existing pavements should be treated as if they are new pavements when predicting the amount of secondary compaction that is likely to result from an increase in wheel loads.
- An ESA approach should be adopted to predict the traffic loading for the design of chipseals to account for increases in mass limits.
- For specific routes with high strength pavements, the damage law exponent used in calculating RUCs could be reduced from the current value of 4. Conversely, low strength low volume pavements should use higher values than 4 for damage law exponents.
- Further pavement modelling work should be conducted to determine appropriate damage law exponents for a greater range of tyre types, loads and pavements. In particular, RLT tests on weaker subgrade materials are required in order to develop an appropriate model for pavements with weak subgrades. If pavement tests for other projects at CAPTIF are appropriate, these models could be further validated then.

Abstract

To improve the efficiency of the road transport industry in New Zealand, a range of mass limit increases for heavy vehicles has been proposed. Some of the options for mass increases include increasing the axle load limit which would inevitably lead to increased road wear.

A range of accelerated loading tests were undertaken, between 2000 and 2004, at the Canterbury Accelerated Pavement Testing Indoor Facility (CAPTIF) to compare the wear generated by different levels of loading. The relative wear in terms of rutting caused by axle loads of 10 and 12 tonnes was compared with that from a standard 8-tonne axle, and the relative rate of surface texture loss between the loads was determined. The higher the pavement's strength, as characterised by its pavement structural number, then the lower the calculated damage law exponent. Conversely, lower strength pavements require a higher damage law exponent.

1. Introduction

1.1 Background

The road transport freight industry in New Zealand understandably wishes to increase its efficiency. Increases in the allowable mass limits for heavy vehicles will achieve this as far as vehicle operating costs are concerned but will rely on the impacts of the changes in mass limits being accurately known. They can then be considered in assigning the new limits and in determining appropriate road user charges (RUC). One of the impacts concerning Road Controlling Authorities (RCAs) is the effect of increasing mass limits on the life of their pavements, and how much more pavement rehabilitation and maintenance will be required.

In response to these probable increases in mass limits on New Zealand roads, a four-year research study at Transit New Zealand's Canterbury Pavement Testing Indoor Facility or CAPTIF (in Christchurch, New Zealand) was undertaken. The study began in 2000 and carried through to 2004, and this concluding report is the last in a series of Transfund New Zealand and Land Transport New Zealand Research Reports which record the research. The other reports are as follows:

- *Transfund New Zealand Research Report No. 214*, by Arnold et al., 2001: Prediction of pavement performance from repeat load tri-axial tests on granular materials.
- *Transfund New Zealand Research Report No. 207*, by de Pont et al., 2001: Effect on pavement wear of an increase in mass limits for heavy vehicles [Stage 1].
- *Transfund New Zealand Research Report No. 231*, by de Pont et al., 2002: Effect on pavement wear of an increase in mass limits for heavy vehicles – Stage 2.
- *Land Transport New Zealand Research Report 279*, by Arnold et al., 2005a: Effect on pavement wear of increased mass limits for heavy vehicles – Stage 3.
- *Land Transport New Zealand Research Report 280*, by Arnold et al. 2005b. Effect on pavement wear of increased mass limits for heavy vehicles – Stage 4.

1.2 The Canterbury Accelerated Pavement Testing Indoor Facility (CAPTIF)

CAPTIF (Figure 1.1) is a 58-m long circular track where the wheelpaths of two vehicles of different loadings can be separated to assess the relative damaging effect of loading parameters on pavements and surfacings. For more detail of CAPTIF see earlier reports of this study (Arnold et al. 2005a, b) and by Pidwerbesky (1995).

Tests were conducted comparing the damaging effect of 40 kN wheel loads (equivalent to a 8.2-tonne dual-tyred axle) with 50 kN and 60 kN wheel loads. The tests were conducted on a limited range of pavements with different aggregate types, thicknesses and surfacings.

Figure 1.1 Transit New Zealand's Pavement Testing Facility, CAPTIF, at Canterbury University, Christchurch, New Zealand.

At the same time that the CAPTIF study was being carried out, ARRB[1] also conducted tests on their Accelerated Loading Facility (ALF) in Australia, in which a range of loads on different pavements were compared.

For the ALF field trials, loads assessed included the current standard 8.2-tonne axle load, a 12.3-tonne axle load and a 16.4-tonne axle load. These were represented by half-axle loads of 40 kN, 60 kN and 80 kN on a standard heavy vehicle dual-tyre arrangement. Results from the ARRB studies are reported in Koh et al. (2002), Vuong et al. (2001, 2003), and Yeo & Alabaster (2003).

The accelerated pavement tests represent a limited number of loading types. Therefore to supplement this study a pavement response study was undertaken. This involved taking measurements of stress and strain within the CAPTIF pavement for a range of different tyre types and pressures. These measurements will enable an assessment to be made of the damaging effect between different tyre types and loads relative to the standard dual-tyred load of 40 kN. Results of this study are reported in Vuong & Sharp (2001) and Arnold et al. (2005a).

As the mass limits research has already been well documented, most of this information is not repeated in this report. Rather the effects of increases in mass limits on pavement (including surfacing) design standards, deterioration modelling, road network impact studies and RUCs are addressed, with a view to developing outputs for implementation.

[1] ARRB – ARRB Transport Research Ltd, Vermont South, Australia.

1.3 Objectives and aims

For the entire mass limits study, the main objectives were as follows.

Overall objectives:

- To determine the damaging effect on pavement wear and chipseal life compared relative to the standard load (of 8.2-tonne dual-tyred single axle) for increases in vehicle loads and tyre pressures via accelerated testing, load response data, existing accelerated pavement test results and the use of an appropriate pavement model.
- To determine appropriate RUCs for new heavy vehicle load limits that will take into account their effects on both pavement and chipseal life.
- To provide a methodology and a pavement model to predict the potential impact on the road network caused by increases in heavy vehicle load limits.

Objectives specific to the 2002/03 CAPTIF tests:

- To determine the effect on pavement rutting of an existing pavement constructed with premium quality materials, when the axle loading is increased from 8.2 tonnes to 12 tonnes (12 tonnes is the limit proposed by the bus industry).
- To measure the pavement response (stresses and strains) under a 12-tonne axle as the pavement deteriorates.
- To investigate the ability of a simple pavement power model to predict life as pavement loads increase.
- To investigate the validity of a simple power model when considering weak (thin) and strong (thick) pavements.
- To predict pavement life from the pavement response data using an appropriate pavement model.
- To determine the relative effect on chipseal life between 8.2- and 12-tonne dual-tyred single-axle loads.

Objectives specific to this report:

This report addresses the methodologies of applying the results from these earlier tests so that increases in mass limits in pavement and surfacing design, deterioration modelling and RUCs can be incorporated. The aims of this report are as follows:

- To summarise the key conclusions and outputs from the research results of the mass limits projects found to date (2005).
- To develop and validate (with CAPTIF data) a pavement model utilising repeated load triaxial (RLT) test results obtained at the University of Nottingham, that allows extrapolation of test results for pavement types and loads not tested at CAPTIF.

- To produce simple power law models to predict the relative damaging effect of different axle loads and different pavement types (e.g. different powers may be needed for weak, medium and strong pavements and/or low, medium or high traffic loads).
- To calibrate New Zealand models for pavement deterioration modelling used in the computer program dTIMS with one or two CAPTIF pavement tests to test their ability to predict deterioration of other CAPTIF tests. To report these results and, if necessary, recommend methods for modifying the dTIMS models (e.g. rutting and texture models) to account for the higher mass limits (e.g. the calculation of SNP (pavement structural number) and traffic loading).
- To analyse the effects of mass limits on the life of chipseal surfacings and recommend changes to chipseal design. (For example, how many equivalent light vehicles (elv) should be used to represent the new higher axle loads, as it is suspected that the current value of 10 requires modification.)
- To assess the impact on the maintenance and rehabilitation costs for the New Zealand road network should the new mass limits be introduced.

This report also aims to assist in the implementation of the results by recommending changes to the following:

- New Zealand Supplement (2005) for the Austroads Pavement Design Guide (1992) to incorporate new higher mass limits for heavy vehicles.
- NZ dTIMS[2] models to incorporate new higher mass limits.
- Chipsealing design to incorporate new higher mass limits.

[2] NZ dTIMS – Deighton's Total Infrastructure Management System for New Zealand conditions.

2. Terminology and assumptions

2.1 Calculating the Damage Law equation

Road traffic consists of a range of vehicle types, wheels and loads. A method intrinsic to pavement design and deterioration modelling is to combine all traffic into one type. This one type of traffic is commonly referred to as an Equivalent Standard Axle (ESA).

The standard axle is defined as a single axle with dual wheels that carries a load of 8.2 tonnes (i.e. a 40 kN dual-tyred half axle as tested at CAPTIF). To calculate the number of ESAs for any given traffic distribution the following equation is used as given in the Austroads Pavement Design Guide (Austroads 1992):

Damage Law equation

$$ESAs = \left[\frac{Actual\_axle\_load}{Reference\_axle\_load} \right]^{n} \qquad \text{Equation 2.1}$$

where:

ESA = number of equivalent standard axles needed to cause the same damage as one pass of the actual axle load (Actual_axle_load, Equation 2.1)

Actual_axle_load
= actual axle load in kN

Reference_axle_load
= reference load depending on the axle load group as defined in Table 2.1

n = damage law exponent (commonly = 4)

Table 2.1 Reference axle loads (Table 7.1 in Austroads 1992).

Axle: Tyres:	Single Single	Single Dual	Tandem Dual	Triaxle Dual
Load (kN)	53	80	135	181

The origins of the Damage Law Equation (Equation 2.1) for combining traffic into one type came from the AASHO[3] (1962) road test which was conducted in the United States (US) in the late 1950s, using roads, vehicles and a climate which bear little resemblance to those in New Zealand today. AASHTO[3] later calculated a damage law exponent of 4 based on a comparison of the number of axle passes required to reach the end of the pavement life for the reference axle and of the number of axle passes required for the axle load in question.

The pavement end-of-life in the AASHO tests was defined by reaching a certain pavement serviceability index value which considers factors such as rut depth, roughness and cracking.

[3] AASHO American Association of State Highway Officials (before 1973). It was superseded by AASHTO American Association of State Highways & Transportation Officials in 1974.

The Damage Law Equation can then be re-written as in Equation 2.2, for the purpose of determining the most appropriate damage law exponent:

$$\frac{N_{40kN}}{N_{L\_kN}} = \left[\frac{P_{L\_kN}}{P_{40kN}}\right]^n \qquad \text{Equation 2.2}$$

where:

- n = the exponent of the power law
- N_{L_kN} = the load cycles of load P_{L_kN} to reach a certain level of wear defined as the pavement's end-of-life
- N_{40kN} = the load cycles of reference load P_{40kN} to reach the same given level of wear defining the pavement's end-of-life as achieved by load P_{L_kN} in N_{L_kN} load cycles
- P_{L_kN} = Actual axle load
- P_{40kN} = Reference load of 40 kN

Taking the logarithm of both sides, the damage law exponent n can be determined (Equation 2.3):

$$n = \frac{log\left(\frac{N_{40kN}}{N_{L\_kN}}\right)}{log\left(\frac{P_{L\_kN}}{P_{40kN}}\right)} \qquad \text{Equation 2.3}$$

The tests at CAPTIF used two higher loads to compare with the standard dual-tyred half axle of 40 kN for the calculation of the damage law exponent. The tests defined that the level of wear when the pavement has reached its end of life was a VSD of 15 mm.

2.2 Measuring Vertical Surface Deformation (VSD)

VSD is more conveniently measured at CAPTIF using the transverse profilometer as it is the maximum vertical difference from the start reference level of the pavement. Further, the measurement of VSD is more stable in comparison to straight-edge measurements that are influenced by shoving on the edges of the wheelpaths. Rut depth is determined using a straight edge across the pavement and incorporates the upward shoving at the edges of the wheelpath (Figure 2.1). However, in the CAPTIF tests the edges moved downwards which distort the straight-edge rut depth as shown in Figure 2.2.

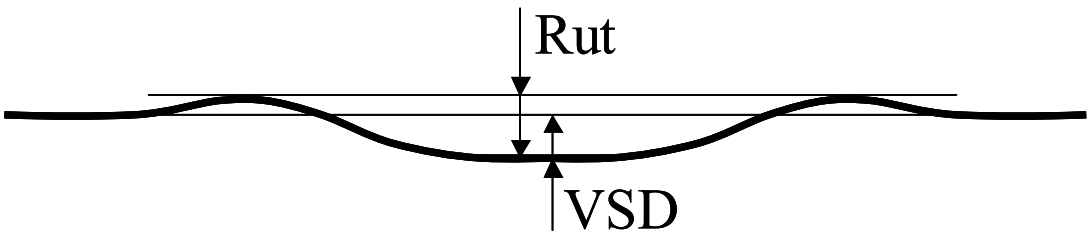

Figure 2.1 The different measures of pavement deformation.

Figure 2.2 shows the comparison of measured VSD and rut depth at CAPTIF, determined mathematically from an imaginary straight edge. The rut depth calculated is less than the VSD value measured at CAPTIF, although the values are expected to be the same early in the pavement lives before shoving occurs. A reason for this is related to the initial reference level taken for calculating the VSD values and how the edges of the ruts at CAPTIF move downwards during the testing which affected the straight-edge rut depth (Figure 2.2).

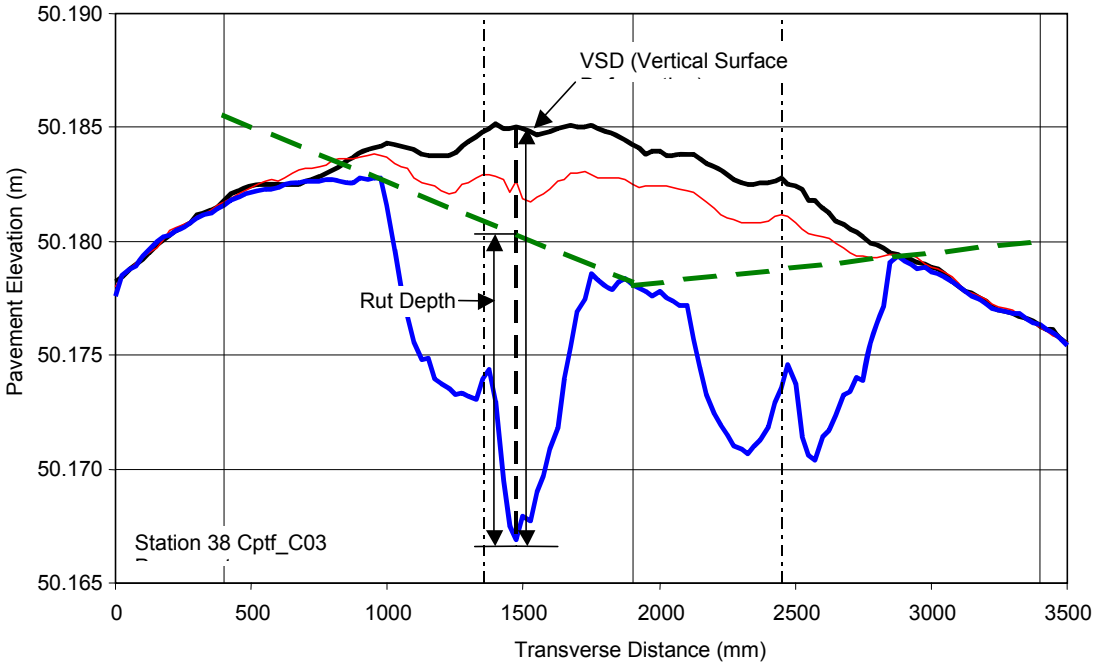

Figure 2.2 Comparison of rut depth and VSD using CAPTIF data.

2.3 Defining pavement end-of-life

In calculating the damage law exponent, the end-of-pavement life needed to be defined for the CAPTIF tests, to enable the number of wheel passes to be determined when the end-of-life of a pavement segment has been reached. The end-of-life has been defined as occurring when 10% of the pavement segment has exceeded a VSD value of 15 mm. Six factors were considered for arriving at this definition:

1. How the pavement's end-of-life is defined for New Zealand state highways;
2. How the CAPTIF test pavements deteriorate;
3. The amount of extrapolation (if any) required so that the CAPTIF data can determine the number of wheel passes to reach the defined end-of-life of a pavement;
4. The different environment of CAPTIF, namely a indoor dry environment and thus no problems of water ponding in the wheelpaths and penetrating the pavement structure;

5. Review of stations where the defined end-of-life was reached and exceeded;
6. The effect of the chosen pavement end-of-life criteria on the calculated damage law exponent.

A range of factors govern a pavement segment's end-of-life on the state highways in New Zealand. Rutting, or VSD as in the CAPTIF pavements, is the only form of deterioration that needs to be considered in Factor 2 above. A rut depth of 20 mm for New Zealand roads is considered a cut-off at which repairs or rehabilitation are required. Further, one-kilometre pavement sections are considered to have reached their end-of-life when at least 10% of the pavement area has met or exceeded the pavement end-of-life criteria (in this case a rut depth $\geq$20 mm).

Considering Factor 3 above is important, as the amount of extrapolation of the data should be minimal to reduce errors. However, the 2003 CAPTIF test results in the heavier wheelpath showed, after 1,000,000 passes (i.e. at the end of the current test), the average VSD (excluding the segment that failed) was 8 mm, while VSDs ranged from 5 mm to 13 mm. The lighter wheelpath resulted in an average VSD of 4.5 mm with a range of 3 mm to 7 mm. Therefore, extrapolation will be required on most VSD measurements. The method employed to extrapolate the VSD data is discussed later.

To minimise errors the amount of extrapolation should be kept to a minimum and perhaps a VSD limit of 10 mm is appropriate. However, a VSD value of 10 mm is considered to be far from the value of 20 mm currently taken to be the end-of-life for New Zealand roads, so a VSD value of 15 mm was considered a comparable value for the pavement's end-of-life at CAPTIF.

A lower value of VSD defining the pavement end-of-life is considered appropriate for CAPTIF because it is an indoor facility and ruts of 10 mm or more would pond water in the field. This water would penetrate into the pavement structure and weaken the material which, in turn, would accelerate the rate of rutting leading to failure. This would not occur for ruts at CAPTIF and the onset to failure would be much later. However as a rut depth of 15 mm in the field would soon spell failure caused by water ingress, then a VSD value of 15 mm at CAPTIF defining the end-of-life is considered appropriate.

On review of a pavement segment progression of VSD where a VSD value of 15 mm was achieved albeit after the second stage of loading, a slight increase in the rate of rutting is shown once a VSD of 15 mm has been reached (see dashed line in Figure 2.4).

Finally, considering that the damage law exponent is a relative effect of two different wheel loads, the chosen VSD is considered to have a marginal effect on the resulting damage law exponent. Figure 2.3 shows the marginal effect of the chosen VSD value on the damage law exponent as found in Stage 3 of the mass limits project at CAPTIF (Arnold et al. 2005a).

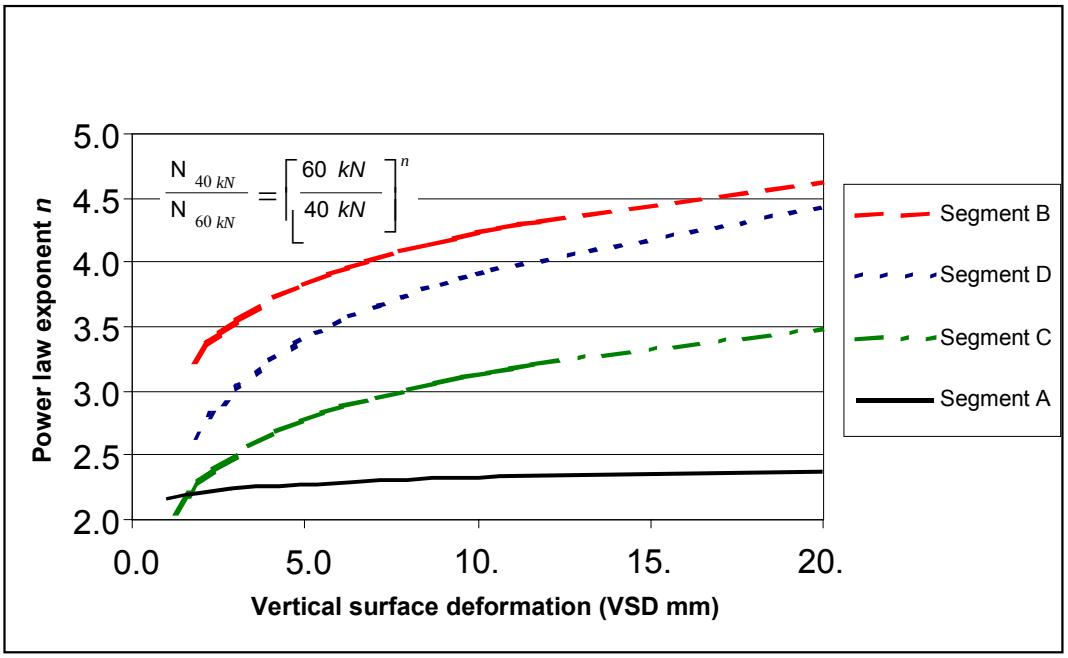

Figure 2.3 Power law exponent *n* determined for a range of vertical surface deformation (VSD) values (after Arnold et al. 2005a).

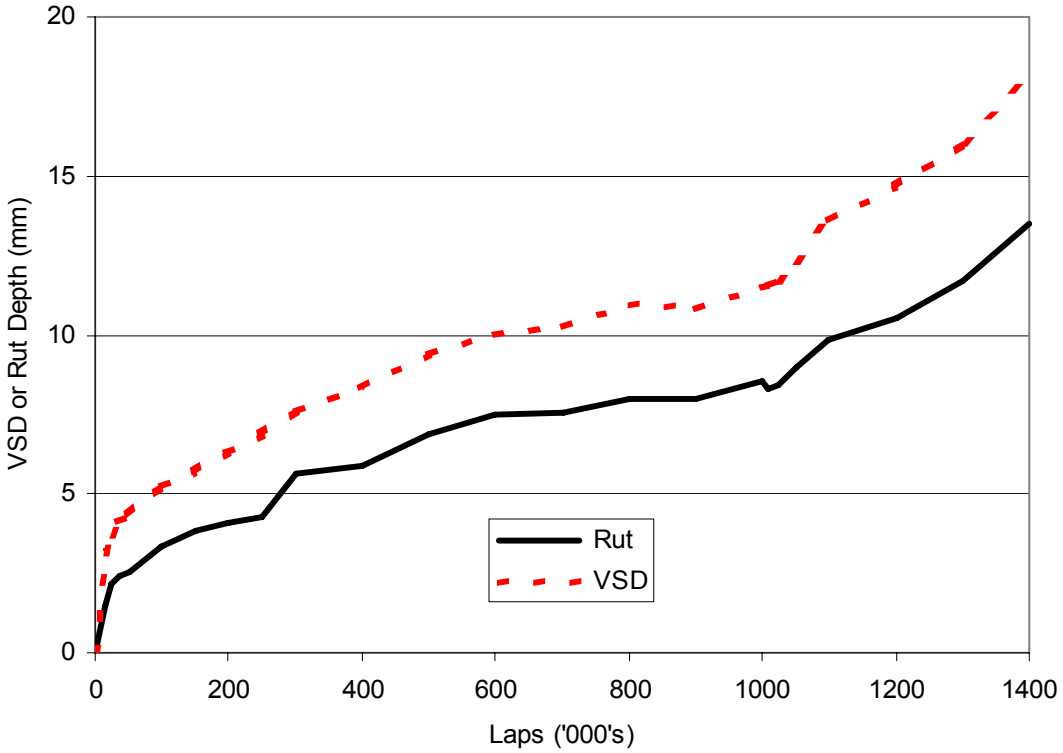

Figure 2.4 Comparison of rut depth and VSD measurements made at CAPTIF.

2.4 Extrapolation using the 10th percentile

For each CAPTIF pavement segment at least 10 measurements of VSD were made at the 1 m stations. The numbers of wheel passes to reach a VSD value of 15 mm were determined for measurements from each station. Finally, the life of the pavement segment was the 10th percentile value or when 10% of the segment has reached the failure criteria. It is realised that the use of percentiles assumes a normal distribution which, for 10 measurements, was likely to not be the case. However, the results do show a spread about the average value, although not strictly as a normal distribution, and the 10th percentile value is consistently near the lowest two values.

As the 10th percentile value is used as a criterion for New Zealand state highways, using the 10th percentile value for the CAPTIF pavement segments is considered appropriate. Further, the 10th percentile value better distinguishes between the performances of the various pavement segments. One reason for this is the effect of dynamic loading present at CAPTIF, in that a weaker pavement will deform first at its weakest location. This depression causes a rise which in turn will cause a higher load at one point but an equal and opposite lighter load at another point. The net effect on a weak pavement segment is that certain stations will rut at a high rate, while an equal number of stations will rut at a much lower rate. Therefore the average rut depth is near that for the other segments for the weaker pavement segment but it will have a greater range of rut depths measured.

Despite these arguments in favour of applying the 10th percentile for extrapolation, it was still considered prudent to include the average value in the analysis for comparison.

2.5 Summary

Determination of the appropriate damage law exponent for increases in mass limits is an important step in calculating RUCs.

Damage law exponents are used in pavement design and in calculating RUCs in New Zealand. Further, deterioration models all use the number of ESAs as an input into the equations that predict deterioration.

3. Pavements used in the CAPTIF tests

3.1 Pavement types

All the pavements tested were of thin surfaced, unbound granular pavements with variations in granular materials and depths. Five different granular materials and two depths were tested at CAPTIF. Only the one subgrade soil type was used, and a similar strength subgrade was used in the ALF tests in Australia. This report summarises the results of all the pavement tests over the past four years and, because similar segment ID symbols had been used in the earlier tests, new segment IDs were assigned as shown in Table 3.1.

Table 3.1 Identification symbols used for pavement segments.

New ID	Original ID	Report used in	Test used in	CAPTIF or ALF
Cptf_A03	A	Arnold et al. (2005a) [Stage 3, RR279]	40 kN cf 60 kN	CAPTIF
Cptf_B03	B			
Cptf_C03	C			
Cptf_D03	D			
Cptf_E03	E			
Cptf_A01	A	de Pont et al. (2001) [RR207]	40 kN cf 50 kN	CAPTIF
Cptf_B01	B			
Cptf_C01	C			
Cptf_D01	D			
Alf_1_03	1	Vuong et al. (2003)	40 kN cf 60 kN	ALF
Alf_2_03	2		40 kN cf 80 kN	
Alf_3_03	3		60 kN cf 80 kN	

The pavements consisted of three layers: the wearing surface; basecourse aggregate; and subgrade (Figure 3.1). Thicknesses and materials used for the various pavement types tested are detailed in Table 3.2. The thicknesses are average representative values to enable classification of the pavement segments. As can been seen, all the pavements have the same medium strength subgrade with pavement depths ranging from 218 to 320 mm. A total of six different aggregates are used, of which four of these are considered premium quality crushed rock. The wearing surface consisted of asphaltic concrete, which was replaced by a chipseal surfacing when texture deterioration was studied.

Compared with the possible pavement types present in the New Zealand state highway network, this accelerated pavement loading set is considered to be fairly limited.

Table 3.2 Summary of characteristics of test pavements.

New ID	Pavement [1]Thickness (mm)	Aggregate Short Description	Basecourse Aggregate Description	Subgrade Type
Cptf_A03	320	Montrose Class 2	20mm max size rhyolite from Montrose, Victoria, Australia	Silty clay (CBR=11%)
Cptf_B03	250			
Cptf_C03	250	AP40 TNZ M/4	40mm max size alluvial gravel, greywacke from Canterbury, NZ	
Cptf_D03	320			
Cptf_E03	320	Rounded AP40 TNZ M/5	40mm max size uncrushed rounded river gravel from Canterbury, NZ	
Cptf_A01	300	AP40 TNZ M/4	40mm max size alluvial greywacke gravel from Canterbury, NZ	
Cptf_B01	300	AP40 TNZ M/4 + fines	40mm max size alluvial greywacke gravel, deliberately contaminated with 10% by mass silty clay fines from Canterbury, NZ	
Cptf_C01	300	Montrose Class 2	20mm max size rhyolite from Montrose, Victoria, Australia	
Cptf_D01	300	Recycled concrete	Recycled crushed concrete from Auckland building demolition sites	
Alf_1_03	235	AP40 TNZ M/4	40mm max size alluvial greywacke gravel from Canterbury, NZ	Imported Sand (CBR=10%)
Alf_2_03	218	Montrose Class 2	20mm max size rhyolite from Montrose, Victoria, Australia	
Alf_3_03	244	Recycled concrete & class 4	20mm max size blend of 50% recycled crushed concrete and 50% Class 4 from Victoria, Australia	

[1] Includes thickness of approximately 25 mm of asphaltic concrete surfacing, or chipseal surfacing where textural deterioration was studied.

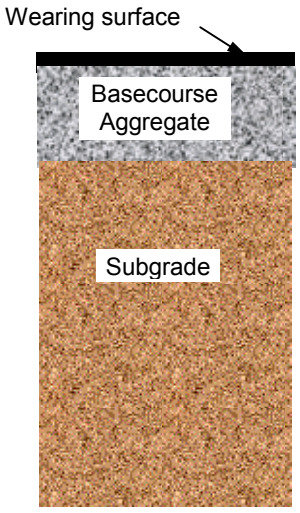

Figure 3.1 Section through test pavement used for CAPTIF tests.

Apart from the two tests with the substandard aggregates (Cptf_E03 and Cptf_B01) similar performances would be expected in the tests. Rounded uncrushed river gravel was used for Cptf_E03 segment while the aggregate used in Cptf_B01 was deliberately contaminated with 10% (by mass) silty clay fines.

3.2 Pavement strength

As discussed, all the pavements should be of similar strength. However quite different performances in terms of rutting and VSD were obtained. These differences in performance appeared to primarily relate to the aggregate type and in part to the pavement thickness.

Falling Weight Deflectometer (FWD) tests were undertaken at regular intervals during testing. The FWD measurements were analysed to determine various pavement strength parameters such as subgrade strain (to calculate pavement life); average pavement modulus/stiffness; structural number; and peak deflection. These parameters were later analysed against actual pavement life at each station, as predicted by the actual measurements of VSD. Results are discussed in Chapter 4.

4. Results and analysis for pavement structure

4.1 Introduction

The results and analyses of the previous stages of the CAPTIF mass limits study are covered more fully in other Transfund New Zealand Research Reports (de Pont et al. 2001, 2002; Arnold et al. 2001, 2005a, b).

Further analysis of the results obtained for each 1-m station (rather than analysing average segment values) is presented in this chapter. The analysis uses a particular pavement strength parameter to predict deterioration in terms of rutting or VSD, and the appropriate damage law exponent. It also deals with the effect on the life of the pavement structure, in terms of rutting, with increases in mass limits. The effect of increases in mass limits on the life of a chipseal surfacing is covered in Chapter 6.

4.2 Pavement life from VSD per station

For each 1-m station in each CAPTIF pavement segment (Table 3.1), VSD (Figure 2.1) was measured at various loading increments up to 1,000,000 loading passes. As discussed in Section 2.2 the value of VSD that governs the end of the pavement life was chosen to be 15 mm. However, a VSD of 15 mm was achieved at only the few stations that failed early. Therefore, the VSD measurements were extrapolated to estimate the number of wheel passes that would occur before the VSD was equal to 15 mm. Two methods of extrapolation of the VSD measurements were employed: a best fit linear projection, and a best fit power model.

Best fit linear projection or compaction–wear model

The best fit linear projection method was applied to the data from 150,000 to 1,000,000 after the initial compaction period. This linear extrapolation is essentially applying the compaction–wear model (Equation 4.1) that has been recommended in the previous reports on the mass limits project (de Pont et al. 2001, 2002; Arnold et al. 2005a).

$$VSD = Comp. + N \cdot Wear \qquad \text{Equation 4.1}$$

where:

- $Comp.$ = a constant value of VSD (mm) to account for the initial compaction that occurs early in the pavement life
- $Wear$ = long-term steady state wear (mm) of VSD per load cycle (mm/N)
- N = number of loading cycles

Best fit power model

The second method used to extrapolate the VSD measurements was a best fit power model of the form shown in Equation 4.2.

$$VSD = a N^{b} \qquad \text{Equation 4.2}$$

where:

- VSD = cumulative Vertical Surface Deformation (mm)
- a, b = best fit regression constants

N = loading cycles

The power model (Equation 4.2) appears to have a better fit to the data, although the linear extrapolation model is considered to be more appropriate for thin-surfaced granular pavements. This is because an ever-reducing rate of rutting (or shakedown) is predicted with the power model (Equation 4.2). However results from research conducted at the University of Nottingham predicted that this is only possible for pavements with a structural asphalt cover of at least 100 mm thickness (Arnold 2004). Further, due to possible water ingress later in a pavement's life, a linear projection maybe more appropriate because it calculates a shorter life.

Reviewing VSD measurements on a station where a VSD of 15 mm had been reached (Figure 4.1) shows that, although initially the rate of rutting decreases, it eventually increases.

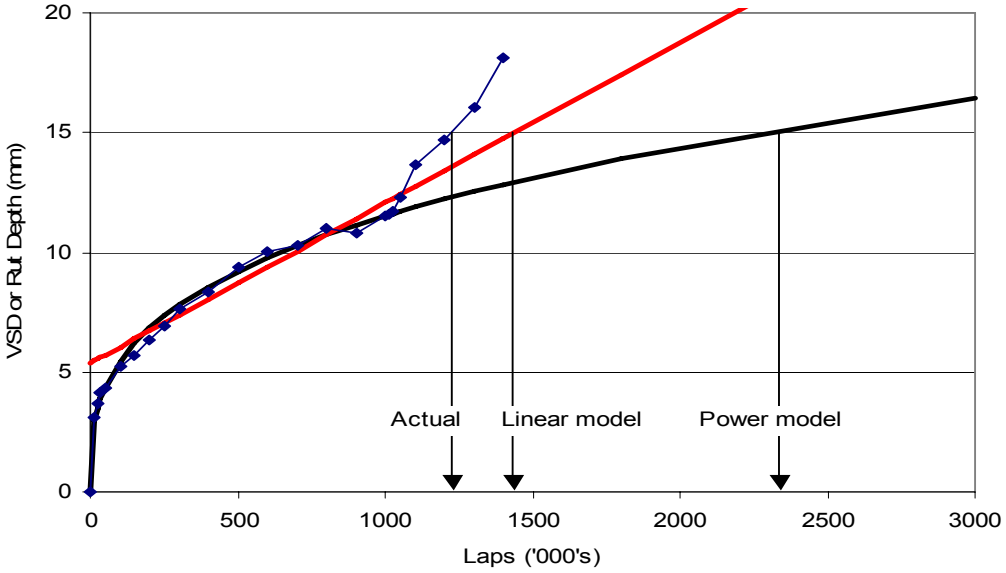

Figure 4.1 Linear and power model extrapolation methods compared to actual results.

Both the linear and power models were fitted to the VSD data for the first 1,000,000 loading cycles for station 38 in Segment Cptf_C03 to check the accuracy of predicting life (i.e. when the VSD = 15 mm). The power model shows a good fit to the measured data for the first 1,000,000 loading cycles but, as can be seen in Figure 4.1, the model is a poor predictor of pavement end-of-life. However, the reverse trend is shown for the linear model where the fit is not as good to the measured data but the predicted life is closer to the actual life. Therefore, a linear extrapolation of VSD data to a value of 15 mm is recommended in order to predict pavement life.

Examples of the pavement life calculation for both the power model and linear model methods are shown in Figures 4.2 and 4.3. They show significant differences in the predicted end-of-life (i.e. when 15 mm VSD has been reached). The biggest difference occurs for the 40 kN wheel load as this has less deformation initially and therefore the power model had more effect by calculating a slower rate of deformation.

Therefore the damage law exponent calculated is also affected by the method of extrapolation employed, with the power model approach resulting in a higher damage law exponent.

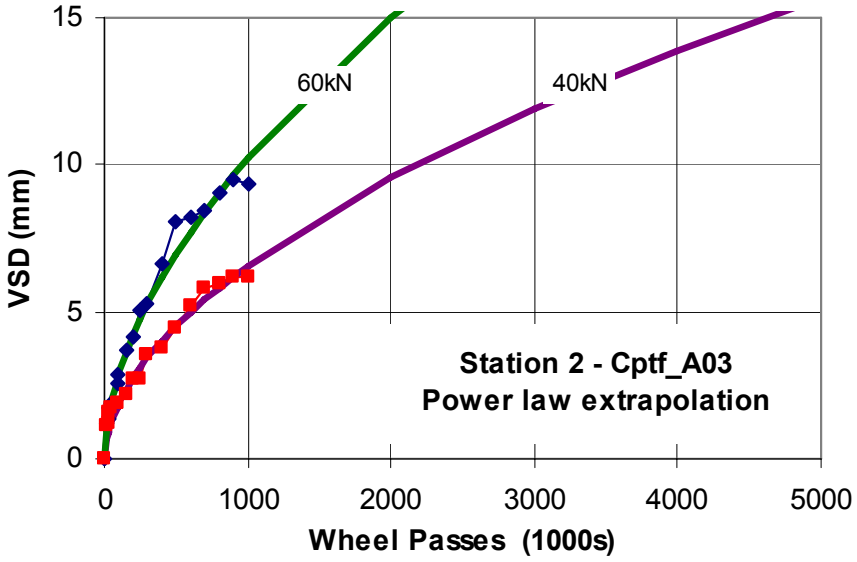

Figure 4.2 Extrapolation of VSD data using the power model.

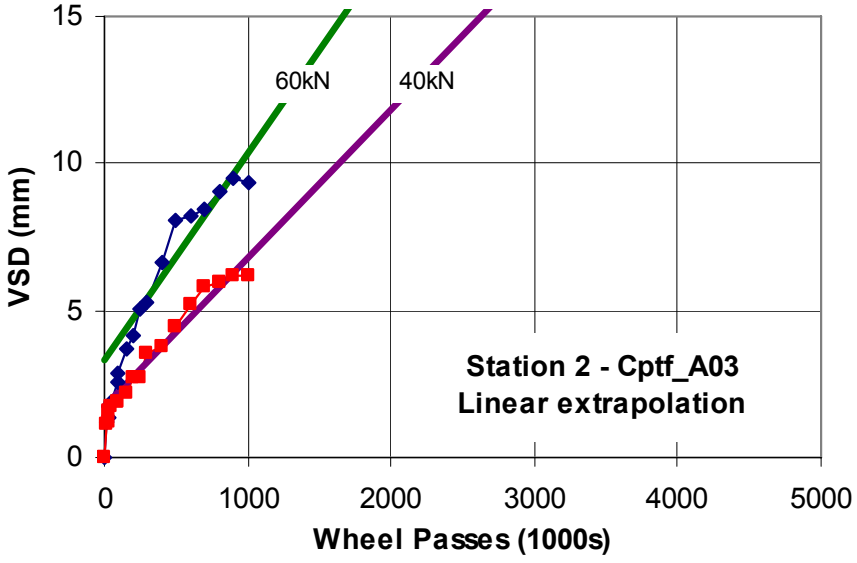

Figure 4.3 Extrapolation of VSD data using the linear model.

Table 4.1 Pavement lives calculated from linear extrapolation of VSD to 15 mm.

ID (Table 3.2)	Load (kN)	Pavement Life in Wheel Passes (10^6) – *Linear*		
		Average	10th %ile	90th %ile
Cptf_A03	40	2.9	2.4	3.4
Cptf_A03	60	1.7	1.3	2.0
Cptf_B03	40	3.0	2.8	3.3
Cptf_B03	60	1.4	1.2	1.6
Cptf_C03	40	2.8	2.4	3.2
Cptf_C03	60	1.4	1.1	1.5
Cptf_D03	40	3.2	2.6	3.8
Cptf_D03	60	1.5	1.2	1.9
Cptf_E03	40	0.8	0.4	1.4
Cptf_E03	60	0.2	0.1	0.3
Cptf_A01	40	4.5	2.5	7.7
Cptf_A01	50	2.3	1.1	3.4
Cptf_B01	40	4.8	2.4	7.8
Cptf_B01	50	2.4	1.3	3.4
Cptf_C01	40	6.4	4.5	8.3
Cptf_C01	50	4.7	2.2	7.5
Cptf_D01	40	6.2	4.3	9.4
Cptf_D01	50	4.2	3.4	5.1

Table 4.2 Pavement lives calculated from power law extrapolation of VSD to 15 mm.

ID (Table 3.2)	Load (kN)	Pavement Life in Wheel Passes (10^6) – *Power*		
		Average	10th %ile	90th %ile
Cptf_A03	40	5.7	3.9	8.2
Cptf_A03	60	1.9	1.4	2.2
Cptf_B03	40	7.0	5.7	8.2
Cptf_B03	60	1.5	1.3	1.8
Cptf_C03	40	6.1	4.6	9.5
Cptf_C03	60	1.7	1.2	2.0
Cptf_D03	40	11.9	5.2	16.3
Cptf_D03	60	2.0	1.4	2.6
Cptf_E03	40	0.5	0.2	0.8
Cptf_E03	60	0.2	0.1	0.3
Cptf_A01	40	41.9	4.1	135.5
Cptf_A01	50	4.7	1.3	9.6
Cptf_B01	40	62.7	3.6	89.6
Cptf_B01	50	10.1	1.8	22.3
Cptf_C01	40	72.1	14.5	213.1
Cptf_C01	50	88.8	2.6	226.3
Cptf_D01	40	85.6	18.8	211.8
Cptf_D01	50	14.1	7.4	23.0

The pavement life for each station in the CAPTIF test segments (Table 3.1) was calculated. The summary of pavement lives calculated for the loads tested, in terms of average, lower or 10^{th} percentile, and upper or 90^{th} percentile values for both the linear and the power model extrapolations, are detailed in Tables 4.1 and 4.2. A common assumption is that the pavement has reached the end of its life when 10% of the road section has failed. Therefore, the life calculated in the lower 10^{th} percentile column are probably the most appropriate as an estimate of life for a segment (Figures 4.4 and 4.5). For the CAPTIF 2001 (e.g. Cptf_A_01) segments some very long lives were calculated using the power model extrapolation for some stations. One reason is because steel suspensions were used on the vehicles in these tests and these caused both high and low loadings at each station.

Results show that Segments Cptf_C01 and Cptf_D01 under 40 kN loads had the longest pavement lives. The Cptf_D01 pavement used recycled crushed concrete which has a slight cementing effect and this could explain the long life achieved. The Cptf_C01 used the Australian crushed rock and the increase in life is because many surfacing repairs were required when delamination had occurred. These repairs smoothed over any rutting that was appearing and so the Cptf_C01 data has been excluded from the database of results. Segment Cptf_E03 of the 2003-year testing at CAPTIF had the shortest life, as was expected, because the aggregate was of poorer quality being a rounded uncrushed material. Based on the discussion and review of pavement-life predictions the linear method of extrapolating VSD data to predict pavement life is recommended and was used in the results and analysis recorded in Chapter 5 of this report.

4.3 Damage law exponent

As discussed in Section 2.1, the damage law exponent is used in pavement design and deterioration modelling. The damage law exponent was calculated from lives predicted when 10% of a segment had a VSD of 15 mm or greater using the linear method of extrapolation (Figure 4.4). Results are shown in Table 4.3 where the Cptf_D01 Segment had the lowest damage law exponent of 1.1. Recycled crushed concrete was used in this segment which, as shown, is insensitive to increases in mass limits.

Table 4.3 Damage law exponent calculated using linear extrapolation for each pavement segment.

ID (Table 3.2)	Exponent *n*
Cptf_A03	1.5
Cptf_B03	2.0
Cptf_C03	2.0
Cptf_D03	1.9
Cptf_E03	3.2
Cptf_A01	3.4
Cptf_B01	2.7
Cptf_C01	3.2
Cptf_D01	1.1

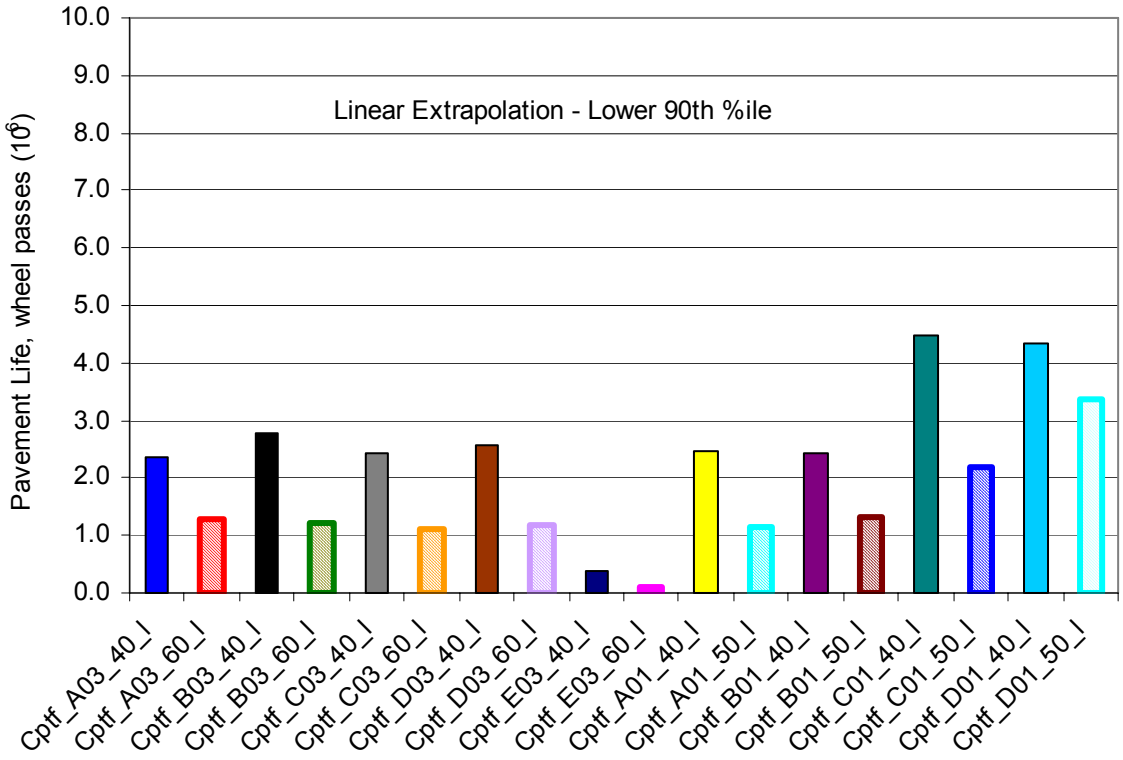

Figure 4.4 10th percentile lives calculated from linear extrapolation of VSD data to 15 mm.

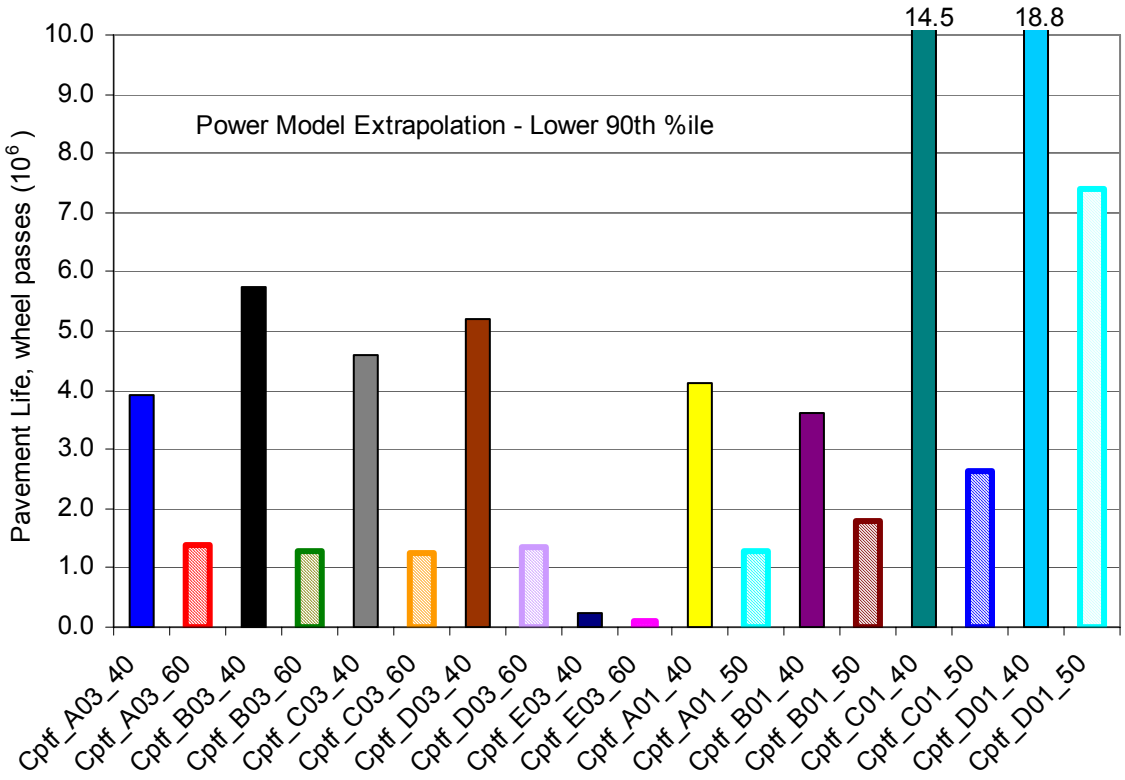

Figure 4.5 10th percentile lives calculated from power model extrapolation of VSD data to 15 mm.

4.4 Pavement life prediction

Pavement life is currently predicted in one of two ways: either by checking the existing pavement against design limits (using Equation 4.3 taken from Austroads 1992); or in deterioration modelling (e.g. Equation 4.4 taken from HDM). Checking against pavement design criteria involves computing the vertical compressive strain in the subgrade and then using this value in a transfer function to calculate life in terms of wheel passes.

Deterioration modelling as used by HDM, requires the pavement structural number (SNP) and the number of ESAs for input into various equations to predict the progression of various deterioration modes such as cracking, potholes, roughness and rutting.

This present project is concerned with determining a method to allow the designer to make accurate predictions of pavement life in design and of deterioration should an increase in mass limits occur. Therefore, the first step in the analysis of the CAPTIF data was to test the current inputs for the prediction of life and deterioration modelling against actual life obtained in the CAPTIF test.

If a method can be developed that will accurately predict pavement life for the 40 kN load case (P_{40kN}) and another load (P_{L_kN}), then these pavement lives (N_{40kN} and N_{L_kN}) can be used to determine the damage law exponent n (see Equation 2.3). The damage law exponent can then be used in pavement design and deterioration modelling for determining the traffic loading in terms of ESAs (Equation 2.1).

The pavements studied at CAPTIF were all tested with the FWD at 1-m stations at wheel loading increments of 0, 50,000, 500,000 and 1,000,000 wheel passes. These FWD results were, effectively, pavement deflections measured directly under the load and at different radial distances from the load. The FWD deflection values were used either directly to calculate the SNP for deterioration modelling or indirectly for determining pavement layer moduli/stiffnesses for pavement design and computation of SNP and subgrade vertical compressive strain.

4.4.1 Subgrade strain (for pavement design)

The FWD measurements recorded at 50,000 load cycles for the pavement segments in the 2003 CAPTIF test were analysed further. At this 50,000 cycle stage of FWD testing, all the pavement segments had not failed (although some sections of Cptf_E03 failed soon after), and the pavement had passed the initial compaction stage. Deflections measured directly after construction are a poor predictor of life because a significant amount of compaction occurs in the early stages of a pavement's life.

The FWD measurements made at this 50,000 stage were back-analysed using the computer program EFROMD2 to determine the pavement layer stiffnesses. Two aggregate layers were assumed in the pavement, while the subgrade was divided into four sub-layers to account for its non-linearity. The back analysis showed that occasionally

maximum and minimum limits were needed on the aggregate moduli to ensure the top layer had the highest stiffness.

After the pavement layer moduli had been deduced, linear elastic analysis with an applied load of either 40 kN or 60 kN was undertaken to compute the vertical compressive strain at the top of the subgrade. The calculated subgrade strain was plotted against the pavement life predicted by the linear extrapolation method as shown in Figure 4.6. Another way to test if the subgrade strain can predict pavement life is plotted in Figure 4.7. This plot shows the calculated life using the Austroads subgrade strain criterion (Equation 4.3) against actual life. The Austroads subgrade strain criterion was found to grossly under-predict the pavement life by between 5 and 200 times less than the actual life.

$$N = \left(\frac{8511}{\mu \in} \right)^{7.14} \qquad \text{Equation 4.3}$$

where:

N = number of wheel passes

μe = vertical compressive strain at top of subgrade (in microstrain)

From this analysis clearly the use of subgrade strain is a poor predictor of pavement life at CAPTIF. One reason is the evidence that, from the post-mortem trenches and research (Arnold et al. 2001), the overlying aggregates have a significant influence on pavement life in terms of their resistance to deformation.

Although the use of subgrade strain is a poor predictor of life, with the exception of two segments, the results show that the Austroads subgrade strain criterion will underestimate the pavement life. The two exceptions were Segments Cptf_A03 and Cptf_E03 in the 40 kN-loaded wheelpath, where the Austroads subgrade strain criterion overestimated the life.

4.4.2 Pavement Structural Number (for deterioration modelling)

The SNP is an indicator of the pavement's life in terms of its resistance to deterioration. This means that pavements with a high structural number can withstand many more loads before failure than pavements with a low structural number. There are many different types of SNP calculations where each method will result in a slightly different value. Therefore, one particular method of SNP calculation is usually recommended by RCAs.

Two methods of calculating SNP were investigated with the CAPTIF data in relation to the actual life predicted from VSD measurements. A relationship should exist similar to that found by Roberts & Roper (1998) (Equation 4.4):

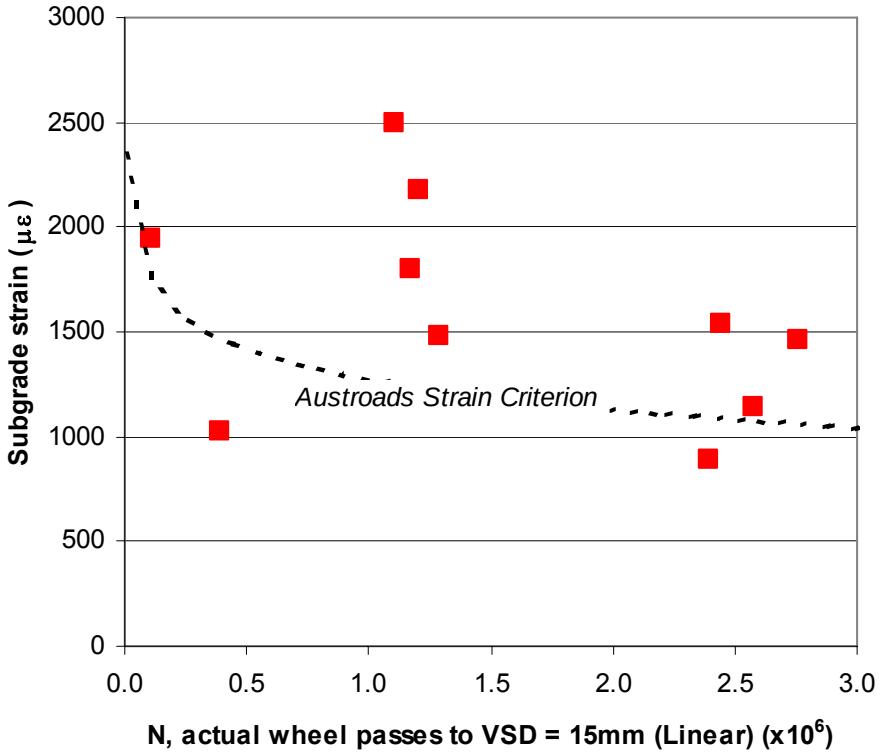

Figure 4.6 Subgrade strain using linear extrapolation at each segment and wheelpath, plotted against pavement life (in number of wheel passes) calculated from VSD data.

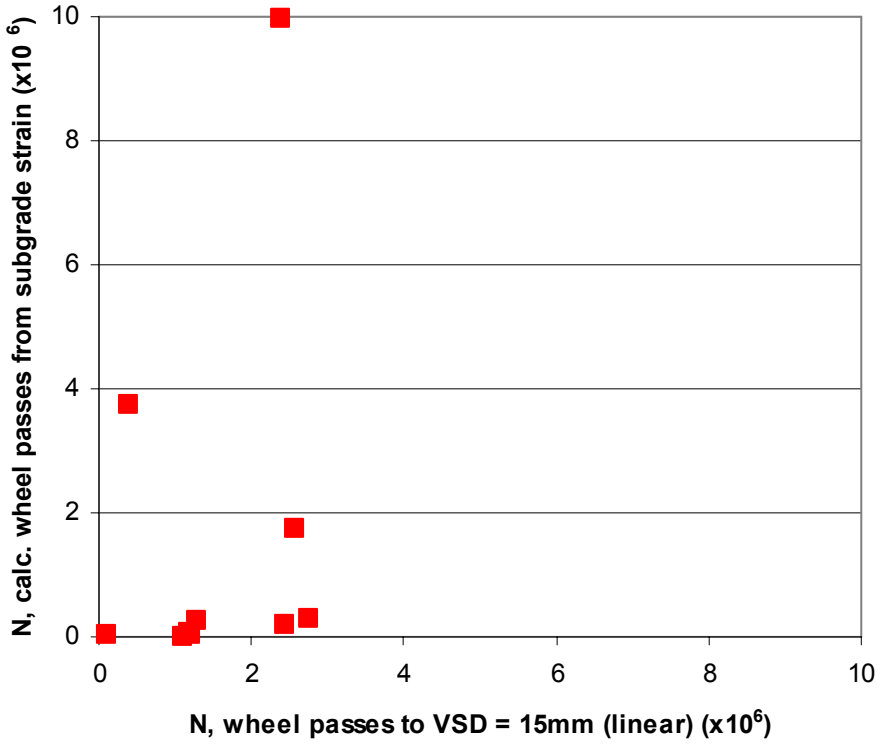

Figure 4.7 Pavement life predicted from subgrade strain compared with actual life (in number of wheel passes) for each segment and wheelpath.

Method 1

$$SNP = 0.6951\ CUM\_ESAL^{0.0993} \qquad \text{Equation 4.4}$$

where:

SNP	=	pavement structural number
CUM_ESAL	=	cumulative number of equivalent standard axles (ESAs)
0.6951	=	constant

Two different pavement structural numbers were calculated for the 2003 CAPTIF pavements for each 1-m station. The first method used to calculate the structural number was a more rigorous approach based on the original HDM-III method. This method uses pavement layer thicknesses and moduli from back analysis of FWD measurements as given by Ioannides (1991). It is the preferred method mentioned in the report '*Implementation of Predictive Modelling for Road Management*' by HTC (1999). The approach fits well with layered elastic theory because the same rational concept relating layer stiffnesses to the cube root of the layer modulus is applied. This rigorous method of SNP calculation is referred to in later plots as '*SNP from moduli*'. Equation 4.5 details how the SNP is calculated from layer thicknesses and moduli.

$$SNP = 0.0394^{\sum_{i=1}^{n\_layer} a_i h_i} + SNSG \qquad \text{Equation 4.5}$$

$$a_i = a_g \left(\frac{E_i}{E_g} \right)^{0.333} \qquad \text{Equation 4.6}$$

$$SNSG = 3.51 \log_{10} CBR - 0.85 (\log_{10} CBR)^2 - 1.43 \qquad \text{Equation 4.7}$$

where:

SNP	=	pavement structural number (Equation 4.5);
a_i	=	layer coefficient for the i'th pavement layer above the subgrade as defined by Equation 4.6;
n_layer	=	number of pavement layers above the subgrade
h_i	=	thickness of the i'th pavement layer
a_g	=	the layer coefficient of standard material (from the AASHO Road Test) as listed in Table 4.4
E_i	=	resilient modulus of the i'th pavement layer
E_g	=	resilient modulus of the standard material (from AASHO Road Test) as listed in Table 4.4
SNSG	=	structural number contribution from the subgrade (Equation 4.7)
CBR	=	subgrade California Bearing Ratio (%)

Table 4.4 Layer coefficients and resilient moduli of standard materials.

Layer type	Layer Coefficient a_g	Resilient Modulus E_g (MPa)
Asphaltic concrete	0.44	3100
Unbound, stabilised basecourse	0.14	207
Unbound sub-base	0.11	104

The subgrade CBR was estimated from the average resilient modulus back-calculated from FWD measurements as per Equation 4.7. This equation is for isotropic moduli as derived from Austroads (1992) where the vertical modulus is 10CBR and the horizontal modulus is half this value. The value of 6.7 in Equation 4.8 is the value derived when converting a vertical modulus to an equivalent isotropic value (i.e. $E_{isotropic}$ = 2/3 $E_{vertical}$). This method resulted in CBR values close to those measured at the test track at the time of construction (i.e. a CBR of 10%)

$$CBR = E_{subg}/6.7 \qquad \text{Equation 4.8}$$

where:

E_{subg} = the average resilient moduli of all the subgrade layers (MPa)

Method 2

Another common method of calculating the SNP is directly from FWD measurements where the pavement thickness and materials used are not known or needed. The formula to calculate SNP as currently recommended by Transit New Zealand is Equation 4.9:

$$SNP = 4.47 + 0.463 \log_e (d_0) + 0.063 \log_e (d_0 - d_{900})^{2.2} - 0.031 \log_e (d_0 - d_{1500})^3 \qquad \text{Equation 4.9}$$

where:

d_0, d_{900}, d_{1500} = deflections in microns at 0, 900 and 1500 mm offsets, under a 40 kN FWD impact load

The average and 10th percentile SNPs were calculated using both methods for the CAPTIF segments. To calculate the SNPs, the FWD data chosen was the first set of full measurements taken after initial trafficking. This was at 50,000 wheel passes for the 2003 data and at 30,000 for the 2001 CAPTIF dataset. The aim was to test the ability to predict the remaining life of the pavement using FWD measurements taken early in the pavement's life. FWD measurements taken immediately after construction are not suitable because a large amount of deformation occurs in the first 30,000 wheel passes.

Summary of Methods 1 and 2

Table 4.5 summarises the SNPs obtained for all the segments. It appears that the use of Equation 4.9 did result in the lowest structural number for Cptf_E03 which had the shortest life (Table 4.1), but only in the heavier wheelpath and if the 10th percentile structural number was used. However, the use of pavement layer moduli to calculate the structural number is considered the most appropriate and its relationship with pavement life and damage law exponent will be investigated further.

Table 4.5 Pavement structural numbers (SNPs) (average, 10th percentile) for all segments, using Equations 4.5 and 4.9.

ID (Table 3.2)	Average				10th Percentile			
	SNP – Moduli Eq. 4.5		SNP Eq. 4.9		SNP – Moduli Eq. 4.5		SNP Eq. 4.9	
	40 kN	60 kN or 50 kN	40 kN	60 kN or 50 kN	40 kN	60 kN or 50 kN	40 kN	60 kN or 50 kN
Cptf_A03	3.7	3.6	2.8	3.0	3.5	3.5	2.8	2.7
Cptf_B03	3.0	3.0	2.4	2.4	2.9	2.9	2.2	2.2
Cptf_C03	3.0	3.0	2.3	2.4	3.0	2.9	2.2	2.2
Cptf_D03	3.3	3.3	2.4	2.5	3.3	3.2	2.3	2.3
Cptf_E03	3.5	3.2	2.1	2.6	3.3	3.0	2.4	1.5
Cptf_A01	2.9	2.9	1.8	2.2	2.9	2.9	1.9	1.6
Cptf_B01	3.0	3.0	2.0	2.3	3.0	3.0	2.0	1.8
Cptf_C01	3.4	3.4	2.5	2.7	3.4	3.4	2.4	2.2
Cptf_D01	3.7	3.7	2.5	2.7	3.7	3.7	2.6	2.1

Analysis of Predictions using SNP

The implementation of NZ dTIMS which models pavement deterioration, has required RCAs to determine the SNPs of road sections in their networks. Therefore, the ability of SNP to predict life and the damage law exponent for increases in mass limits has been investigated with the CAPTIF data.

The first type of analysis compared the 10th percentile SNP with the pavement segment lives determined from the linear method of extrapolation (Figure 4.8). For comparison of the 2001 and 2003 CAPTIF test sections the 50 kN wheel load in the 2001 tests was converted to an equivalent number of 60 kN wheel passes. This conversion used the damage law equation with the appropriate damage law exponent for the segment determined for the 40 kN and 50 kN wheel loads. The solid squares (■) in Figure 4.8 represent the Cptf_E03 segment where some stations failed completely within the first 250,000 loads and were repaired, and it is, in some cases, a significant outlier. This indicates that the method of calculating the SNP and/or the FWD may not locate potential weak pavement areas. Relationships of SNP with pavement life are generally non-existent except, in part, in the heavily loaded wheelpath. This suggests that pavements have to undergo significant loading before the FWD can detect differences in pavement strength.

The number of ESAs are also an important input in deterioration models. Equation 2.1 was used to calculate the ESAs, and the second type of analysis, using the most appropriate damage law exponent (Table 4.3) for the axle load being considered, will improve the result. Damage law exponents were calculated for all the CAPTIF segments comparing the 10th percentile lives from the linear extrapolation method (Table 4.3).

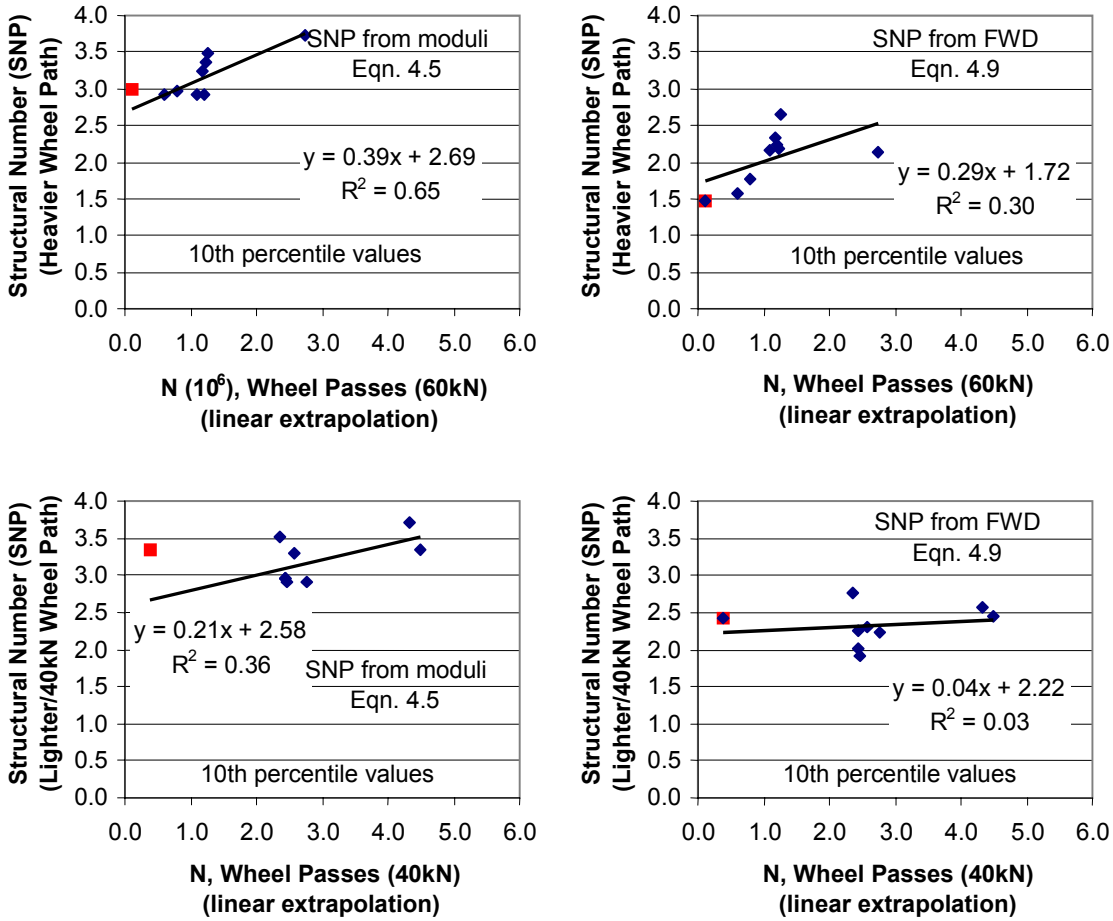

Figure 4.8 10th percentile SNP compared with pavement segment lives from linear extrapolation of VSD to 15 mm, for both heavy (50-60 kN) and lighter (40 kN) loaded wheelpaths. (■ = Cptf_EO3 segment)

These exponent values were plotted against the 10th percentile SNP as shown in Figure 4.9. Relationships are best in the heavier wheelpath and, with the exception of the Cptf_E03 segment (■ solid squares), the more rigorous method using pavement layer moduli to calculate the pavement structural number is best. The rigorous method of SNP calculation uses coefficients that are based on the pavement material type. The assumption is that premium quality basecourse was used in all segments, because in a real situation the type of material is not always known. Should the appropriate layer coefficient value be used for the Cptf_E03 segment, then the SNP calculated would be lower.

The general trend of results shows that, as the SNP reduces, the damage law exponent increases, and the pavement life reduces. These trends are more apparent using structural numbers and lives determined in the heavier (60 or 50 kN) wheelpaths.

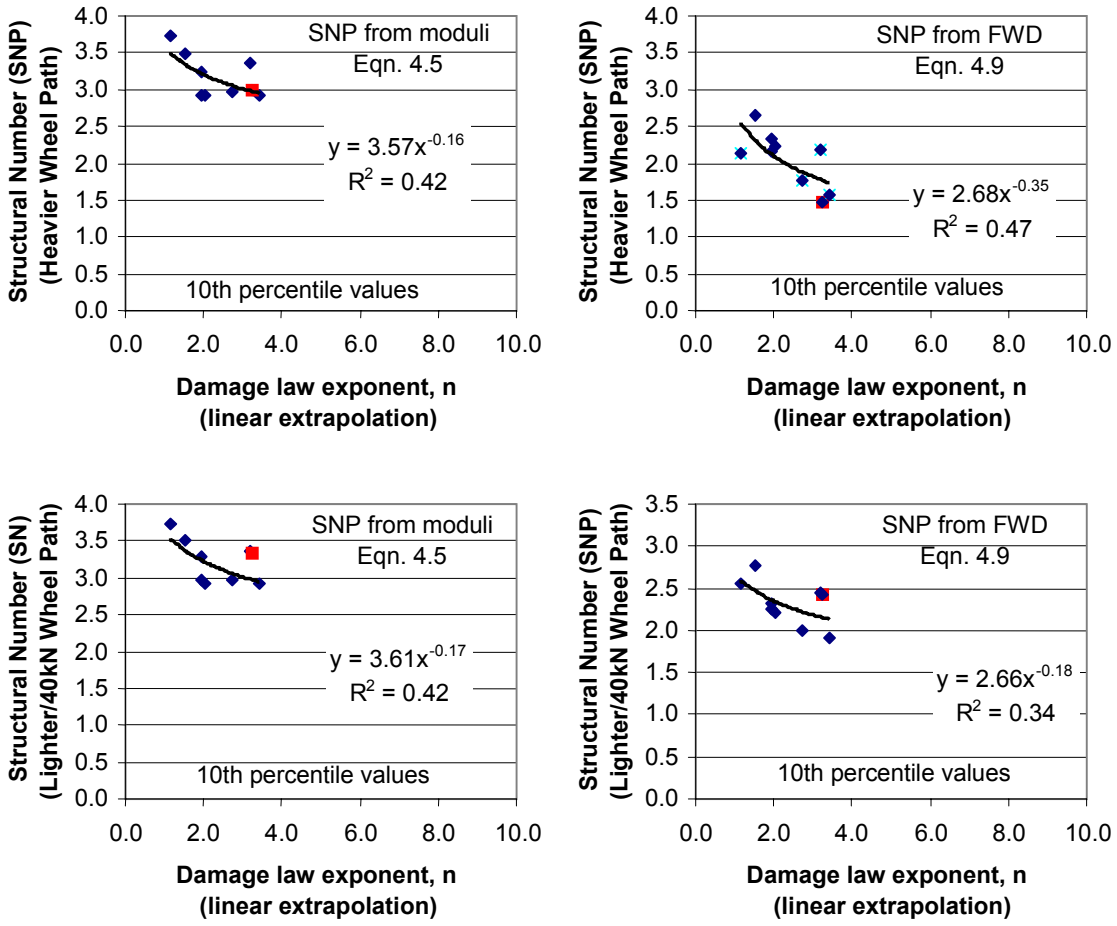

Figure 4.9 Damage law exponent (from Table 4.3) plotted against structural number (SN) for both the heavy (50 or 60 kN) and light (40 kN) loaded wheelpaths.
(■ = Cptf_EO3 segment)

The plot showing the damage law exponent against the SNP calculated from pavement layer moduli in the heavier wheelpath was examined further. The aim is to determine a useful relationship for predicting the damage law exponent based on the SNP. Two sets of analyses were undertaken of this data. The first set of analyses used all the data points (Figure 4.10) while the second excluded a point that was considered as an outlier. This outlier was the point from pavement segment Cptf_C01, which had had several surfacing repairs. The repairs had affected the VSD measurements, and thus affected predictions of life for the two wheelpaths. Further, the VSD measurements in the Cptf_C01 segment showed the unusual result of higher VSD measurements in the lighter (40 kN) for most stations. Removing the outlier (Cptf_C01) improved the correlation, achieving an R^2 of 0.68 (Figure 4.11). A power model was chosen because a better regression is obtained and negative values of the exponent *n* are not possible.

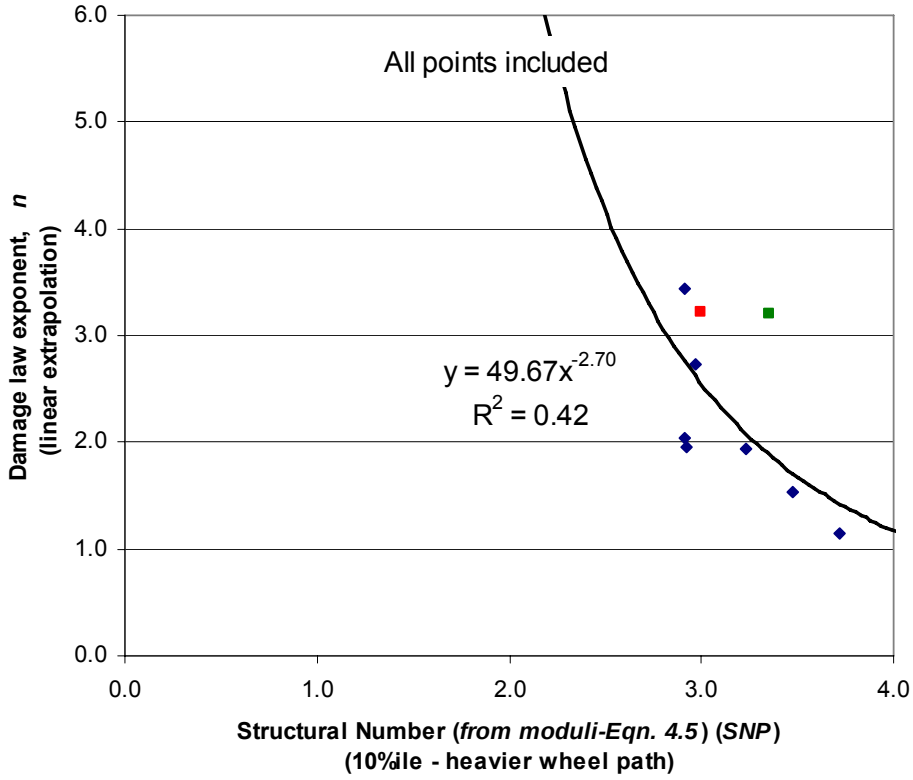

Figure 4.10 Relationships between 10th percentile structural number (SNP) and damage law exponent (*n*) with all data points included (solid squares are outliers).

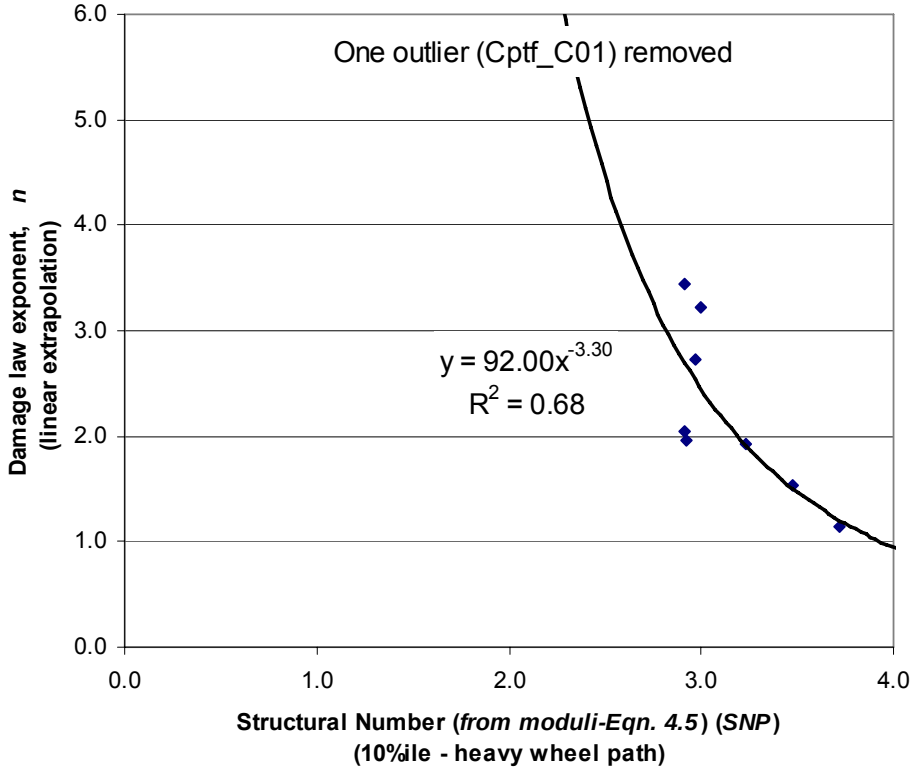

Figure 4.11 Relationships between 10th percentile structural number (SNP) and damage law exponent (*n*) with the Cptf_C01 data point removed.

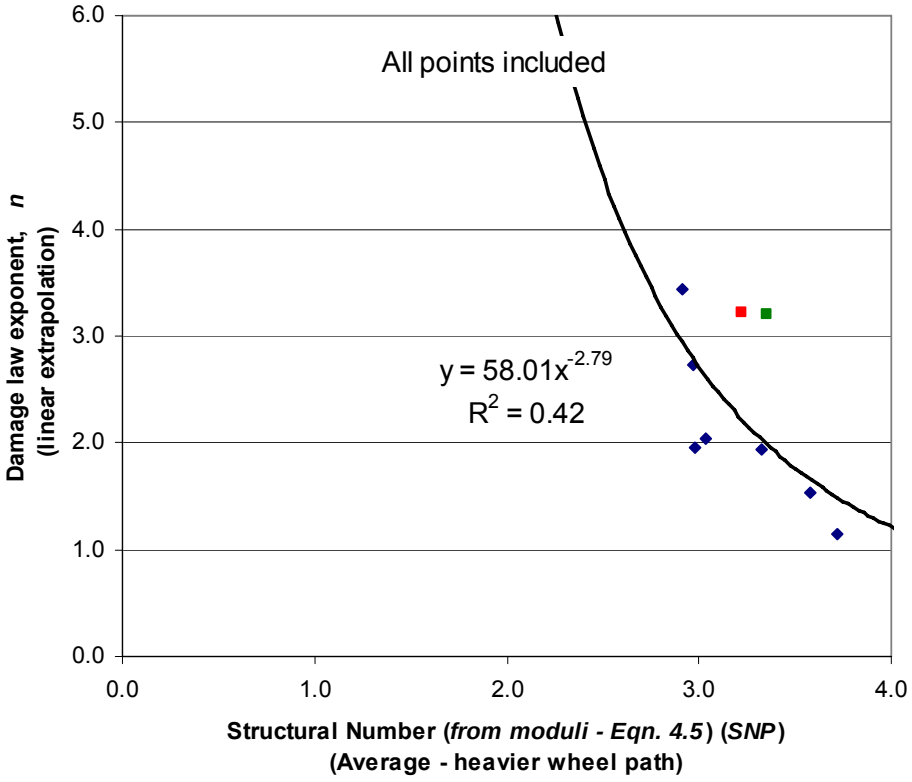

Figure 4.12 Relationships between average structural number (SNP) and damage law exponent (n) with all data points included (■ solid squares are outliers).

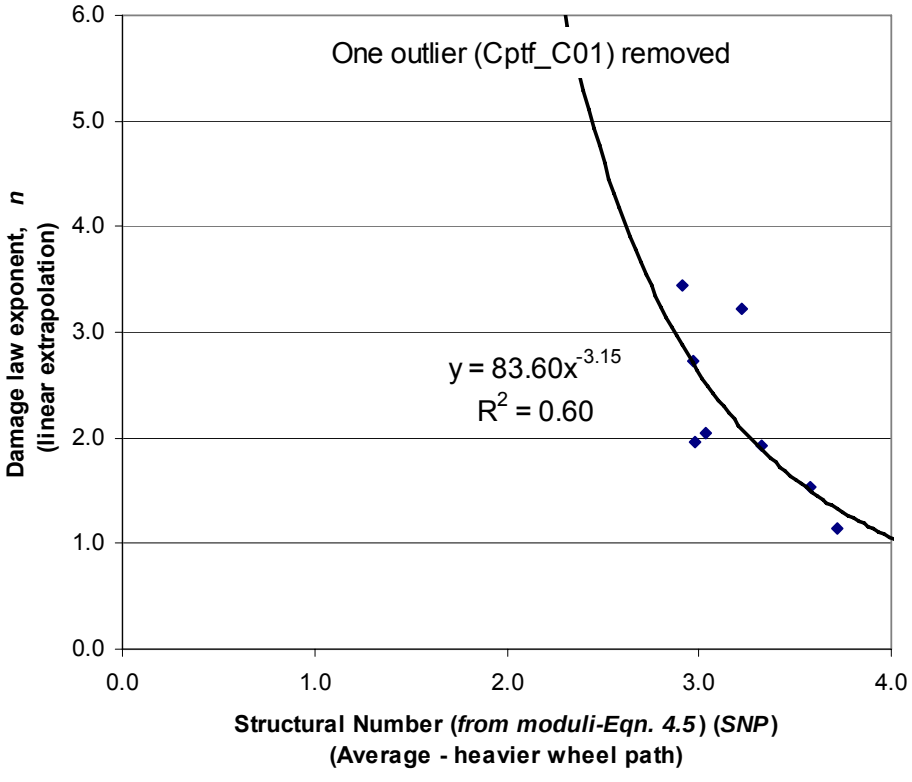

Figure 4.13 Relationships between average structural number (SNP) and damage law exponent (*n*) with the Cptf_C01 data point removed.

Currently in deterioration modelling, the average structural number is used in the models for prediction. We do not recommend using the average structural number as it fails to pick out poorly performing road sections that have a high variation in SNP even though the average value of those variations is acceptable. This is the case for the poorly performing Cptf_E03 segment. This pavement will invariably result in a high roughness because of the large variation in rutting that occurs. Nevertheless, relationships between average structural number and damage law exponent *n* were produced as shown in Figures 4.12 (full dataset) and 4.13 (Cptf_C01 data point removed).

SNP was also calculated directly from the FWD-measured deflections using Equation 4.8. This method enabled the identification of the Cptf_E03 segment as a weak section (i.e. with the lowest SNP), which was the case (i.e. its heavy wheelpath failed at 87,000 wheel passes). However, repeating the analysis above found that, in order to achieve reasonable relationships of SNP and damage law exponent n, Segments Cptf_C01 and Cptf_D03 needed to be excluded. Analysis also showed that the weak Segment Cptf_E03 could be included in the dataset. As discussed, the reason to exclude Segment Cptf_C01 was due to surfacing repairs. Recycled crushed concrete aggregate that has a cementing action was used in segment Cptf_D01 which maybe a reason for the differences in behaviour to the other standard unbound granular pavements. Relationships found between SNP determined directly from FWD measurements and damage law exponent are shown in Figure 4.14. By excluding the two outlier data points, the result shows very good correlations. Further, the use of FWD measurements directly into Equation 4.9 has advantages because the additional step of back-analysis to determine pavement layer moduli from FWD measurements is not needed.

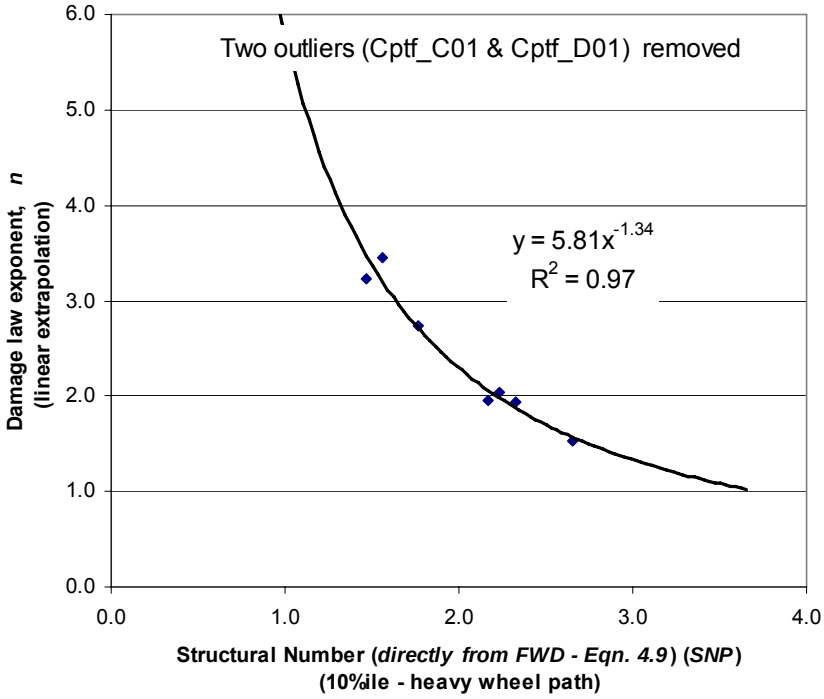

Figure 4.14 Relationships between 10th percentile structural number (SNP) calculated directly from FWD measurements and damage law exponent *n*, with two outliers removed.

Although not reported here, this analysis was repeated using the average SNPs calculated directly from FWD measurements. Three segments, Cptf_D01, Cptf_C01 and Cptf_E03, had to be excluded in order to obtain reasonable correlations. Effectively the use of average SNPs did not detect the weak segment Cptf_E03 and is therefore not recommended.

Summary

A range of relationships were determined between SNP determined by two different FWD methods and the damage law exponent. Reasonable relationships could be determined from SNPs calculated from FWD measurements in the heavier wheelpath against damage law exponents determined from pavement lives and by linear extrapolation of the VSD measurements at CAPTIF.

To confirm if a linear rate of rut progression is an appropriate assumption, the high speed rutting data over the past few years should be examined in another project.

It is recommended that the design for a new pavement in which the layer moduli are estimated, the damage law exponent *n* for loads in excess of the standard load (Table 2.1) should be calculated using Equation 4.10 as in Figure 4.11. For predictions of deterioration on the existing road network from FWD measurements the use of Equations 4.9 and 4.11 (Figure 4.14) would provide the most appropriate damage law exponent. However, these relationships may be modified after reviewing the results from the pavement modelling (see Chapter 5) and RCAs may wish to take a cautionary approach.

$$n = 92.0\ SNP^{-3.3} \qquad \text{Equation 4.10}$$

and

$$n = 5.81\ SNP^{-1.34} \qquad \text{Equation 4.11}$$

where:

n = damage law exponent (Equation 2.1)

SNP = 10^{th} percentile SNP determined from pavement layer moduli using Equation 4.5

Results show that, for low SNPs or weak pavements, the damage law exponent predicted is high (>4). Practitioners would agree with this trend as local roads that are weak would fail quickly with the introduction of new vehicles with increased mass limits. Further, the expected trend is that the strong pavements (high SNP) on the busiest state highways would feel little structural impact with the introduction of increased mass limits. This trend is also predicted by Equations 4.10 and 4.11 as a strong pavement would result in a low damage law exponent, *n*.

Although the results match expectations they are from a very limited number of pavement types and should be used cautiously. Pavement modelling (Chapter 5) for prediction of rut depth validated from the CAPTIF trials will give an indication whether or not these results can be extended to other pavement types not tested at CAPTIF (e.g. a pavement with a weak subgrade).

4.5 Initial deformation

Generally without exception, a significant amount of wheelpath rutting occurs during the first 150,000 wheel passes on a new pavement. This initial rutting can be as much as half the total rutting or VSD that occurs after 1,000,000 wheel passes. Increases in loading also caused an initial amount of deformation, as was found at CAPTIF. In the 2003 CAPTIF tests, the lighter (40 kN) wheelpath was loaded to 60 kN after 1,000,000 passes, and a further 400,000 wheel passes were applied.

A typical example of the initial deformation that resulted from the increase in load is shown in Figure 4.15. This sudden increase in deformation or rutting caused by an increase in mass limits is significant and should be considered when predicting the effect on the road network should an increase in mass limits be allowed.

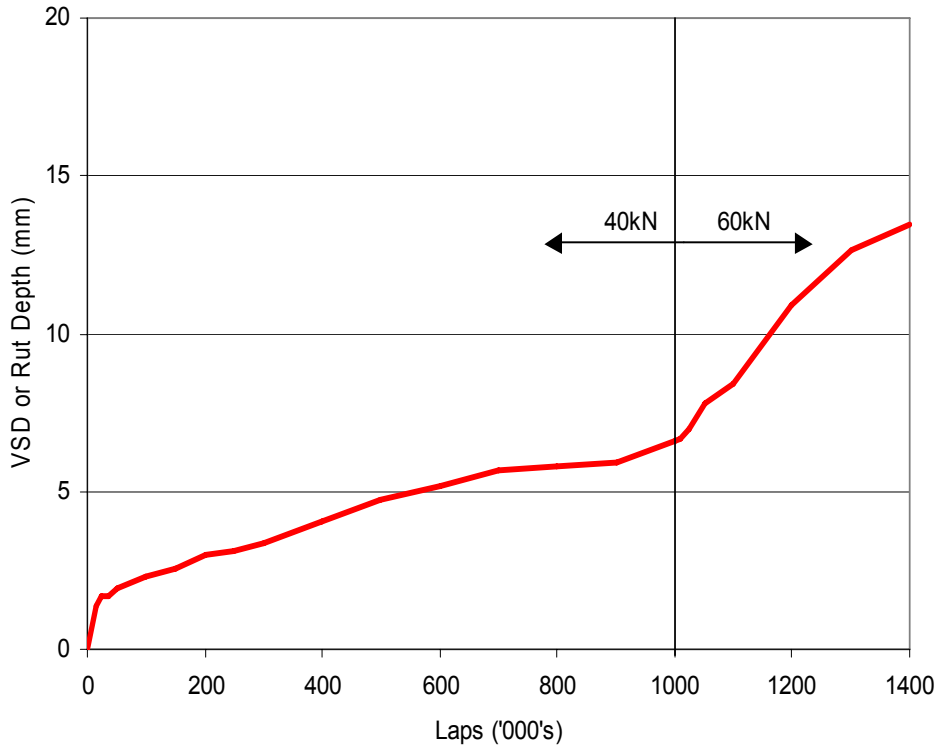

Figure 4.15 Effect on VSD or rut depth of increasing the wheel load from 40 kN to 60 kN after 1,000,000 wheel passes.

In theory should the correct damage law exponent *n* be used to calculate the number of ESAs (Equation 2.1) for the new increase in mass limits, then this initial deformation is taken into account. However, the current form of deterioration modelling would not take into account the initial deformation that would occur after a sudden increase in load. Rather, the steady state condition in terms of the rate of rutting per year would be predicted from the new ESAs calculated per year, but the initial increase in rutting that also would occur cannot be predicted.

In deterioration modelling using dTIMS, the HDM-III (Paterson 1987) model is used to predict the amount of rutting that occurs. These HDM models consist of two components: an initial amount to account for secondary compaction that will occur in the first 1 or 2 years, and an incremental amount of rutting that occurs each year. Effectively, the HDM-III model for the compaction component (*Comp.*) is a constant (*K*) multiplied by the number of ESAs as shown by Equation 4.12.

$$Comp. = K\,N\,(P_L/P_{std\_L})^n \qquad \text{Equation 4.12}$$

where:

$Comp.$	=	the rut depth due to secondary compaction
K	=	constant
P_L	=	axle load
P_{std_L}	=	standard axle load
n	=	damage law exponent
N	=	number of wheel passes of axle load P_L

Assuming that, before any increases are made to mass limits, the axle load P_L is the same as the standard axle load, P_{std_L} (e.g. 8.2 tonne dual-tyred axle), then the ratio of the compaction component of a new load to the compaction component of the previous standard load can be determined from the following Equation 4.13.

$$\frac{Comp._L}{Comp._{Std\_L}} = \left(\frac{P_L}{P_{Std\_L}}\right)^n \qquad \text{Equation 4.13}$$

The CAPTIF data were analysed to determine the appropriate damage law exponent *n* in Equation 4.13. This value is assumed to be the same as that determined from the pavement lives (Table 4.3). Results are plotted in Figure 4.16 and, as can be seen, the damage law exponent values from the compaction components are nearly the same as that obtained for the pavement lives with exception of two data points. These two data points were from pavement segments Cptf_C01 and Cptf_E03 where the results of the initial deformation in both light and heavy load-wheelpaths were nearly the same. The Cptf_E03 segment showed very little initial deformation in both wheelpaths but developed a rapid rate of rutting that resulted in early failure of a number of stations in less than 250,000 wheel passes.

As discussed earlier, pavement-surfacing repairs affected the VSD measurements for the Cptf_C01 pavement. Further, the lighter (40 kN) wheelpath showed higher VSD values than the heavier (50 kN) wheelpath in the Cptf_C01 pavement which resulted in the negative exponent value. Therefore, excluding Cptf_C01 and Cptf_E03 (solid squares) from these results was considered appropriate.

Results of this analysis shows that the HDM-III equation for calculating the initial rut depth caused by secondary compaction for new pavements, using the correct value of ESAs, should be adequate. However, the correct damage law exponent based on the pavement's strength (Equation 4.9 or similar) should be used for the calculation of ESAs. Then to calculate the initial deformation caused by an increase in mass limits on an existing road, simply subtract the compaction component that has been calculated using the loading before an increase in mass limits, from the compaction component calculated

for the new higher loads. The result should be a conservative estimate, as the existing road would have already undergone secondary compaction.

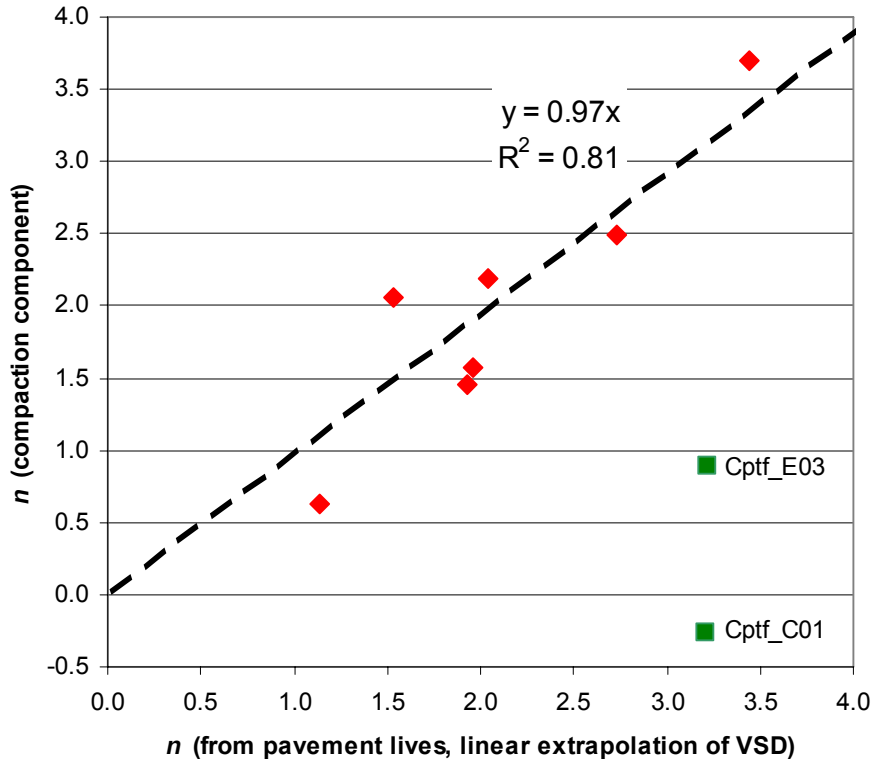

Figure 4.16 Comparison of damage law exponents determined from initial deformation ratios (measured by compaction) and from pavement lives. (■ = Cptf_EO3, Cptf_CO1)

To check if this method of predicting initial rutting caused by a change in loading is conservative, the CAPTIF results from the 2003 and 2001 tests were reviewed as follows.

The 2003 test results for 1,000,000 wheel loadings of 40 kN and 60 kN, then the results after the 40 kN load was increased to 60 kN and a further 400,000 passes were applied.

The 2001 test results for 1,000,000 wheel loadings of 40 kN and 50 kN, then the results after the 40 kN load was increased to 50 kN and a further 320,000 passes were applied.

Results were reviewed by using the slope of the VSD curve for the heavier wheelpath (50 kN or 60 kN) to determine the intercept back from the 1,400,000 (2003 tests) or 1,320,000 (2001 tests) measurements to the 1,000,000 vertical axis. The VSD at 1,000,000 was subtracted from this intercept value and was compared to the difference in intercept values for the two wheelpaths at the beginning of the test. This method of analysis is best explained graphically in Figure 4.17.

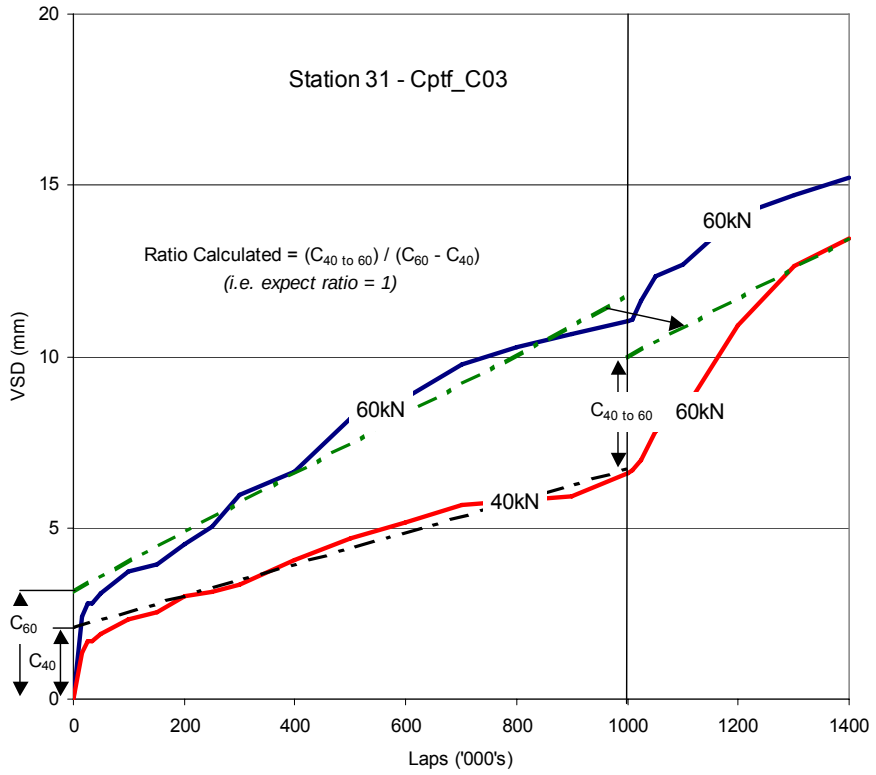

Figure 4.17 Methodology used to validate method to predict initial compaction caused by a change (C) in load (from 40 kN to 60 kN) on an already trafficked pavement (Station 31 of Cptf_C03 segment).

Figures 4.18 and 4.19 show results in terms of ratios of actual additional compaction caused by the increase in load from 40 kN to 50 or 60 kN, to the differences in compaction that occurred at the beginning of the test (i.e. Ratio Calculated, Figure 4.17). This result is, in effect, validating or otherwise the value of compaction that would be predicted using the HDM-III approach. Ratios less than 1 in Figures 4.18 and 4.19 indicate that the HDM-III approach is conservative, and this is shown for most of the segments.

The negative ratios of relative compaction shown in Figure 4.18 for Cptf_A03 and Cptf_B03 indicate that an increase in load on these two segments did not result in the additional compaction that was expected. Reviewing the VSD results on station 4 in Cptf_A03, as shown in Figure 4.20, confirms this to be the case. However, the opposite occurs for the other segments where up to a 4-fold increase in compaction occurred on an already trafficked pavement, in comparison to the difference in compaction between the lighter (40 kN) and heavier (50 or 60 kN) wheelpaths that occurred on a newly trafficked pavement. It is unclear why there were two opposite trends in results, and the significance of the initial compaction that may or may not occur on an existing pavement requires further investigation.

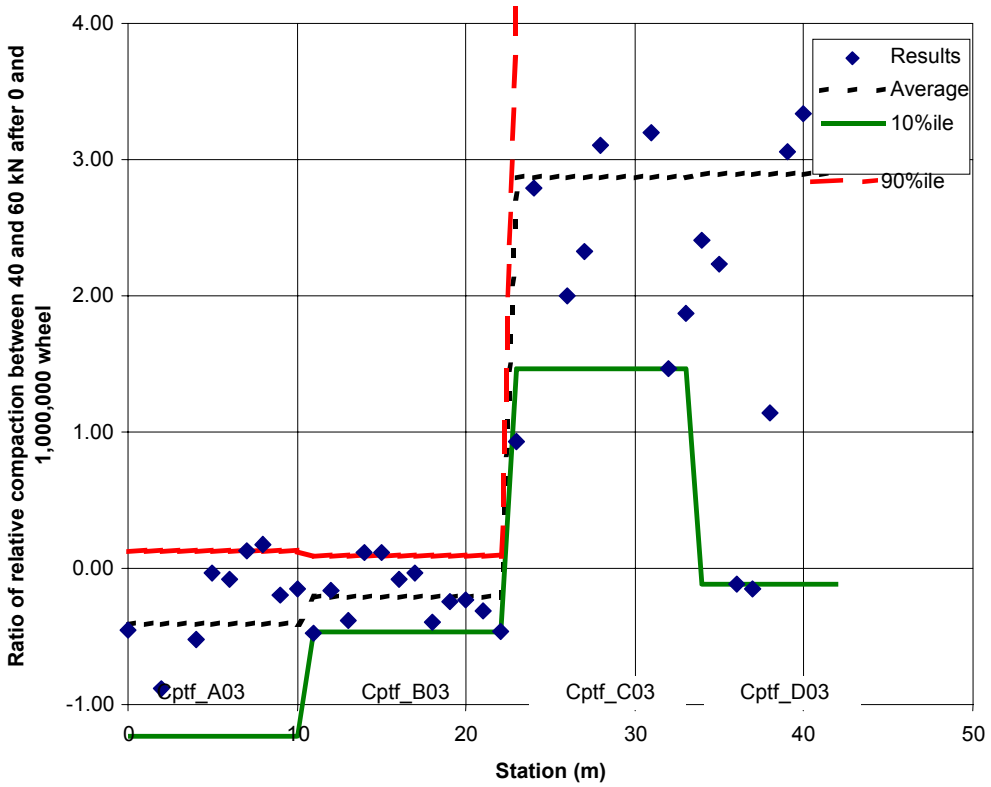

Figure 4.18 Ratio of relative compaction (i.e. Ratio Calculated in Figure 4.17) for the 2003 CAPTIF tests.

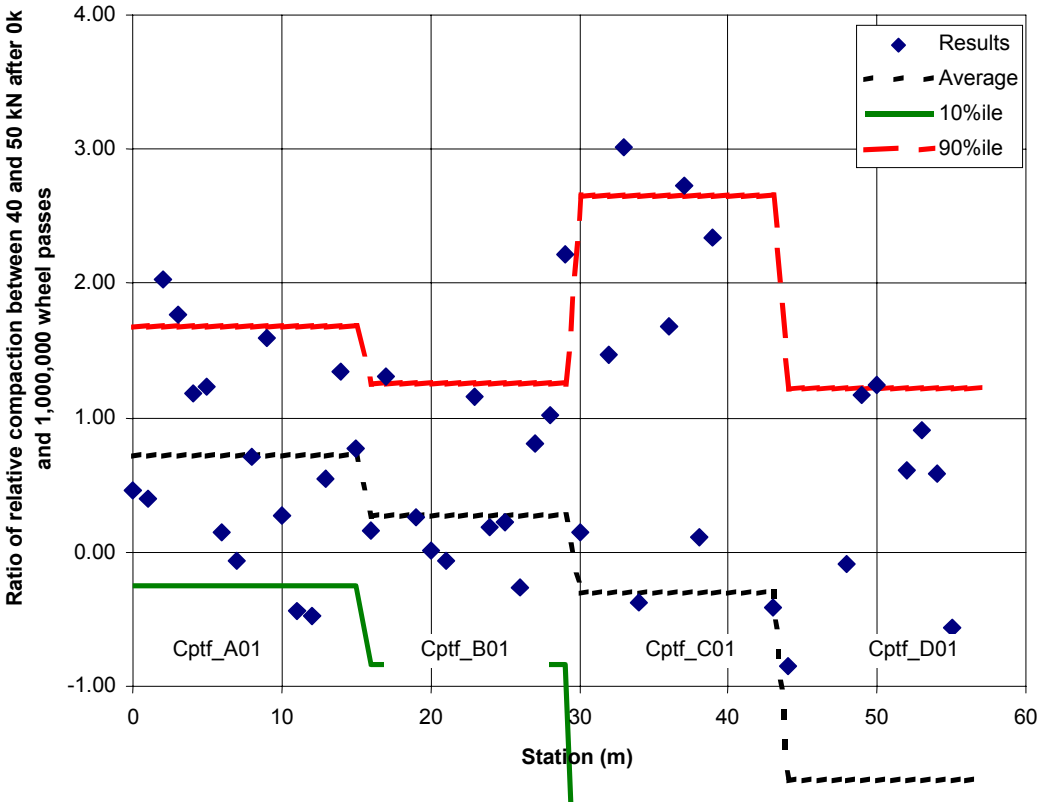

Figure 4.19 Ratio of relative compaction (i.e. Ratio Calculated in Figure 4.17) for the 2001 CAPTIF tests.

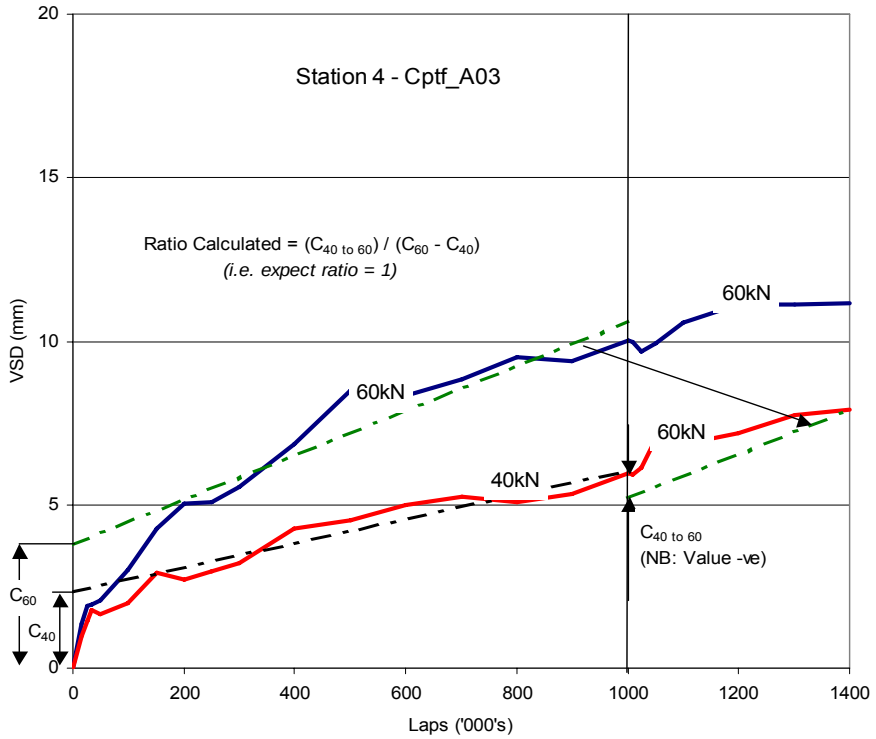

Figure 4.20 Effect of increase on VSD for station 4 in Cptf_A03 segment.).

Reviewing Figures 4.18 and 4.19 suggests that the additional compaction component caused by an increase in load is the same as that which originally occurred for the 50 kN (2001 tests) or 60 kN (2003 tests) loads (e.g. C_{60} = $C_{40\ to\ 60}$, Figure 4.17). To check if this is the case, the ratio of compaction that occurred on an already trafficked pavement ($C_{40\ to\ 60}$, Figure 4.17) to compaction on a new pavement (C_{60}, Figure 4.17) for the 50 kN and 60 kN wheel loads was determined. Figures 4.21 and 4.22 show that results from Cptf_A03 and Cptf_B03 segments did not undergo any additional compaction related to an increase load. However, Cptf_C03, Cptf_D03, Cptf_A01, Cptf_C01 and Cptf_D01 segments predicted that the amounts of compaction that had occurred on an already trafficked pavement were up to twice that had occurred as indicated with the 90th percentile value. On average however, the amounts of compaction on both new and already trafficked pavements are the same for these segments.

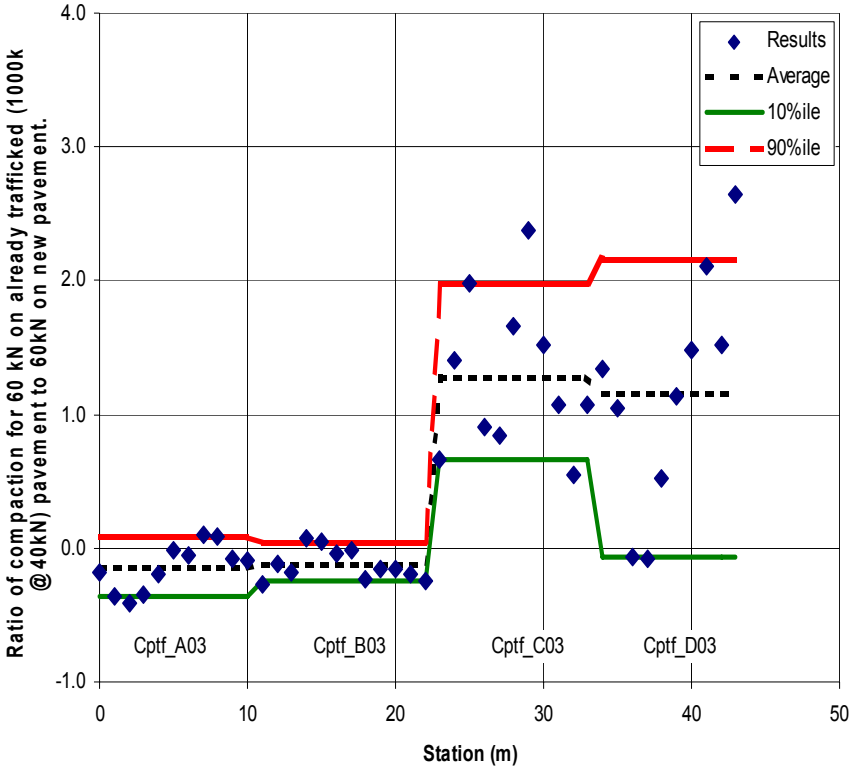

Figure 4.21 Ratio of compaction that occurred on an already trafficked pavement to compaction on a new pavement for the 2003 CAPTIF tests.

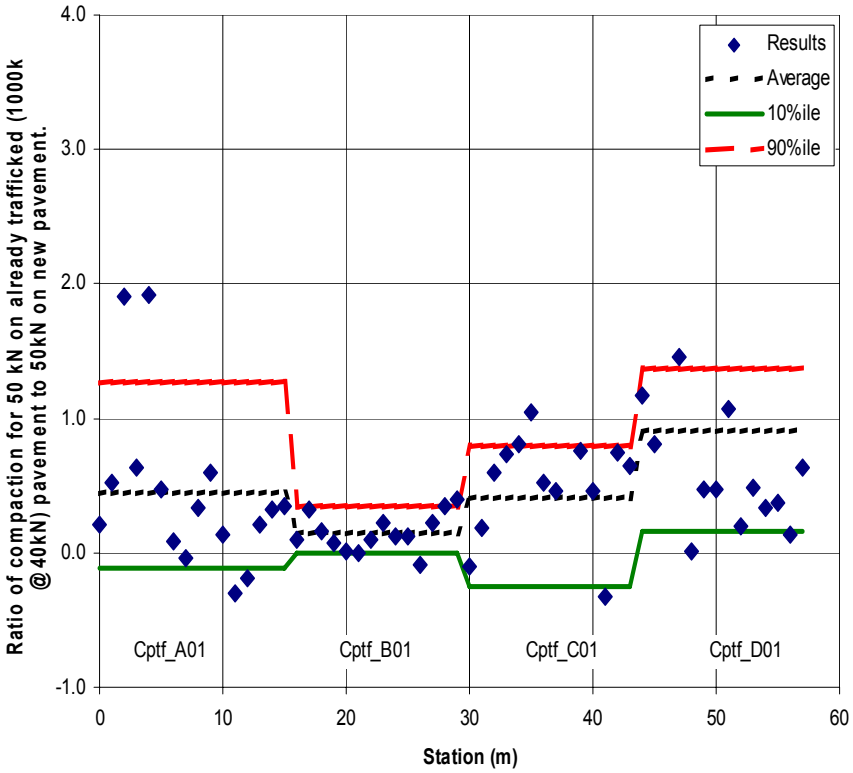

Figure 4.22 Ratio of compaction that occurred on an already trafficked pavement to compaction on a new pavement for the 2001 CAPTIF tests.

4.6 Summary

Results from this study on the initial compaction or rutting that could occur on an existing (i.e. already trafficked) pavement caused by an increase in mass limits show two opposing results. Either no initial compaction or rutting will occur, or the initial rutting can be as much as twice which had occurred on a new pavement. A possible reason for these two different results is the type of aggregate used.

For example, the segments that showed no additional rutting caused by an increase in load were constructed with either the Australian Montrose Class 2 aggregate (Cptf_A03, Cptf_B03) or a New Zealand AP40 complying with TNZ M/4 but with 10% silty clay fines added (Cptf_B01).

The Cptf_C03 and Cptf_D03 segments, which showed up to twice the amount of initial rutting compared with the new pavement, were both constructed with a New Zealand AP40 complying with TNZ M/4. It is unclear why this difference in performance occurred.

Other factors, such as the FWD results at 1,000,000 cycles, could be analysed to determine if the pavement strength influenced the amount of additional rutting caused by a change in load.

In the meantime, it is recommended that, should an increase in loading occur, the existing pavement should be analysed as a new pavement. Also the amount of additional compaction that could occur is predicted using either the HDM-III equation, or another method based on the ESAs calculated using a damage law exponent appropriate to the pavement strength.

When modelling the effect of an increase in mass limits, it may be simpler to factor up the number of ESAs in the first one or two years. This can be calculated by determining the number of ESAs from the steady state model which calculates the amount of rutting per year that is needed to achieve the rut depth calculated from the compaction component. This value of ESAs can then be fed into the deterioration models for other pavement defects such as roughness and cracking.

5. Modelling for pavement structure

5.1 Background

The results of the accelerated pavement testing provided data on only a small range of pavement types. Pavement depth ranged from 250 mm to 320 mm, and the one silty clay subgrade of CBR=11% was used for all the tests. As discussed in Chapter 4, only two different loads (50 kN and 60 kN) were tested to compare with the standard half-axle dual-tyred load of 40 kN, although nationally, pavement types and vehicle loads vary substantially to those tested at CAPTIF. As it is unrealistic to test at CAPTIF the full range of loads and pavement types, a pavement model was used to predict pavement performance in terms of vertical surface deformation for other pavement types.

5.2 Repeated Load Triaxial tests

The pavement model chosen was developed by Arnold et al. (2004). This model utilises the results from many permanent strain repeated load triaxial (RLT) tests undertaken at the University of Nottingham on the aggregates used at CAPTIF. The repeated load triaxial apparatus approximates the loading that occurs on a pavement material element as a vehicle passes. Figure 5.1 illustrates a typical RLT apparatus test set up, for which cylindrical samples of soils or granular materials are used. The number of load cycles is defined by the user, and the axial load type is usually programmed as a sinusoidal vertical stress pulse with a short rest period. Although possible with some RLT apparatuses, for the tests undertaken on the CAPTIF aggregates the cell pressure was not cycled simultaneously with vertical load but held constant. Resilient and permanent strain tests are usually conducted on the same sample.

Many combinations of vertical and horizontal stress conditions occur within a pavement. As each RLT permanent strain test for 50,000 loading cycles at one stress condition takes 2 days (1 day to prepare the sample and 1 day to test), then in order to cover a full range of possible stress conditions, multi-stage tests were undertaken. This involves using one specimen to test a range of stress conditions, where each next stress condition is slightly more severe than the previous. The results of RLT tests were analysed to produce permanent strain rates (% per 1,000,000 cycles) for different stress conditions defined by mean principal stress, p (Equation 5.1) and principal stress difference, q (Equation 5.2).

The pressure which causes volume change in the sample is defined as:

$$p = \frac{1}{3}(\sigma_1 + \sigma_2 + \sigma_3) \qquad \text{Equation 5.1}$$

$$q = \sigma_1 - \sigma_3 \qquad \text{Equation 5.2}$$

where:

p	=	mean principal stress (MPa)
q	=	shear stress invariant, known as deviator stress or principal stress difference (MPa)
σ_1, σ_2, σ_3	=	principal stress components

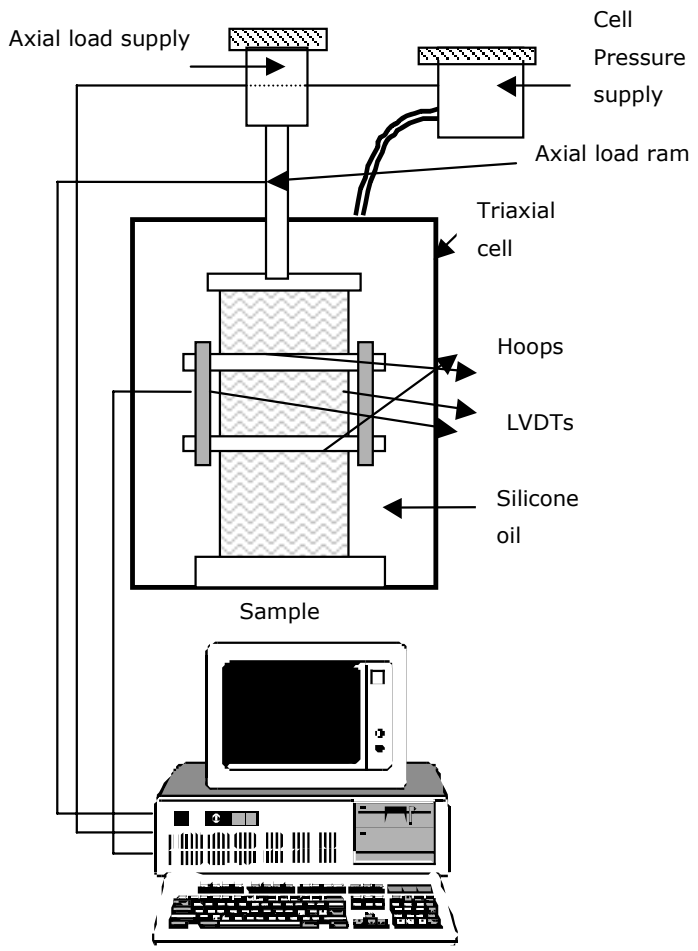

Figure 5.1 The Repeated Load Triaxial (RLT) apparatus used for the CAPTIF tests.

The RLT results for the Australian aggregate (Montrose Class 2) used in the Cptf_A03, Cptf_B03 and Cptf_C01 pavement segments are shown in Table 5.1. These results are reported in two strain rate values for each particular stress condition. RLT tests at each stress level were for 50,000 loading cycles, and to determine the average change in permanent strain from 25,000 to 100,000 and from 100,000 to 1,000,000, the RLT cumulative permanent strain values were extrapolated to 1,000,000 loads. The extrapolation method used was a power model as this provided the best fit to the measured data. Dividing the RLT permanent strain data into only two average permanent strain rates was to minimise the computational effort because, for each permanent strain rate, new constants for the model (see Section 5.3) are required.

Table 5.1 RLT results for tests on Australian Montrose Class 2 aggregate.

ID	RLT test sequence	*p* (MPa)	*q* (MPa)	Permanent strain rate	
				25,000 to 100,000 % per 1,000,000	100,000 to 1,000,000 % per 1,000,000
A03	1a	0.075	0.037	0.022	0.006
	2a	0.075	0.135	0.170	0.030
	3a	0.075	0.181	0.246	0.047
	4a	0.075	0.204	0.378	0.445
B03	1b	0.150	0.135	0.062	0.010
	2b	0.150	0.274	0.295	0.085
	3b	0.150	0.318	14.126	14.612
C01	1c	0.250	0.375	0.191	0.073
	2c	0.250	0.420	0.299	0.087
	3c	0.250	0.469	0.673	0.299
	4c	0.250	0.517	1.203	0.539
	5c	0.250	0.562	3.465	1.806

5.3 Pavement model

In order to determine permanent strain rates at stress conditions in the pavement other than those tested (Table 5.1), a model was fitted to the data. This model was determined by regression analysis of stresses *p* and *q* with the natural logarithm of the strain rate. It is not based on any fundamental behaviour of the pavement materials but was found through trial and error as providing the best fit to the measured data. The result of this analysis of the data is an equation requiring the stress conditions *p* and *q* as inputs defined as:

$$\varepsilon_{rate} = e^{(a)}\, e^{(bp)}\, e^{(cq)} - e^{(a)}\, e^{(bp)} \qquad \text{Equation 5.3}$$

where:

- e = 2.718282
- ε_{rate} = permanent strain rate defined as % permanent strain per 1,000,000 load cycles
- a, b, c = constants obtained by regression analysis fitted to the measured RLT data (e.g. Table 5.1)
- p = mean principal stress (MPa) (Equation 5.1)
- q = mean principal stress difference (MPa) (Equation 5.1)

The silty clay subgrade used at the CAPTIF test track was also tested in the RLT apparatus. This subgrade has relatively high strength with a CBR of 10%. As RLT tests were not conducted on other subgrade types, and in order to model pavements on a weak subgrade, the RLT results for the CAPTIF subgrade were modified to reflect a result that may be expected for a subgrade of half the strength. The principal stress difference, *q*, was simply taken as half the value obtained for the high strength CAPTIF subgrade. This approximation of a weak subgrade has not been validated and it is recommended in

future research that RLT multi-stage permanent strain tests should be conducted on weak subgrades with a CBR of 5% or less.
Constants for Equation 5.3 that were used to estimate the permanent strain rates were determined for the aggregate and subgrade materials, and are given in Table 5.2. For the subgrade material, the model did not provide a good fit to the RLT tests undertaken at a mean principal stress, *p*, of 0.250 MPa. Therefore, constants were obtained for the CAPTIF RLT data that excluded points where the mean principal stress was 0.250 MPa or greater. This was considered acceptable as, at the subgrade level of the pavement, the mean principal stress is generally always less than 0.150 MPa.

Table 5.2 Constants for model (Equation 5.3) to calculate permanent strain rate (% per 1,000,000 load cycles).

Constants	Aust. Montrose Class 2		CAPTIF Subgrade		Weak Subgrade (CBR 5%)	
	25,000 to 100,000	100,000 to 1,000,000	25,000 to 100,000	100,000 to 1,000,000	25,000 to 100,000	100,000 to 1,000,000
a	−2.393	−3.592	2.125	−0.744	2.125	0.7436
b	−23.1996	−31.203	−22.583	−15.567	−22.583	−15.567
c	16.7943	21.329	9.564	9.273	19.127	18.546

The goodness of fit of Equation 5.3 to the measured data for the basecourse aggregate and subgrade is shown in Figures 5.2 and 5.3 respectively. Because of the small dataset (although large considering the expense of conducting RLT tests), the correlations are low. However, visibly the model fits the data well and shows the correct trend. Results from the RLT tests (Arnold et al. 2004) show, for a certain value of mean principal stress, there is a maximum value of principal stress difference, *q*, before sample failure occurs. The model does not have a limit to the maximum value of *q* but rather it will return a very high permanent strain rate value.

To determine the total permanent strain for any given number of load cycles and stress condition, three values of permanent strain are added together (Equation 5.4). The first is a compaction component to account for the deformation that occurs in the first 25,000 loads (Equation 5.5), the second is the amount of permanent strain to occur from 25,000 to 100,000 loads (Equation 5.6), while the third is the remaining permanent strain that occurs from 100,000 to N loads (Equation 5.7).

To calculate the compaction component, the RLT test data was analysed. The average ratio of permanent strain that occurred in the first 25,000 loads to the average permanent strain rate from 100,000 to 1,000,000 loads in units of % per 1,000,000 loads was determined. There was significant scatter in the ratios calculated but the average for both the aggregate and subgrade materials was 0.25. Therefore, a value of 0.25 was used for *C* to determine the amount of deformation to occur in the first 25,000 loads as per Equation 5.5.

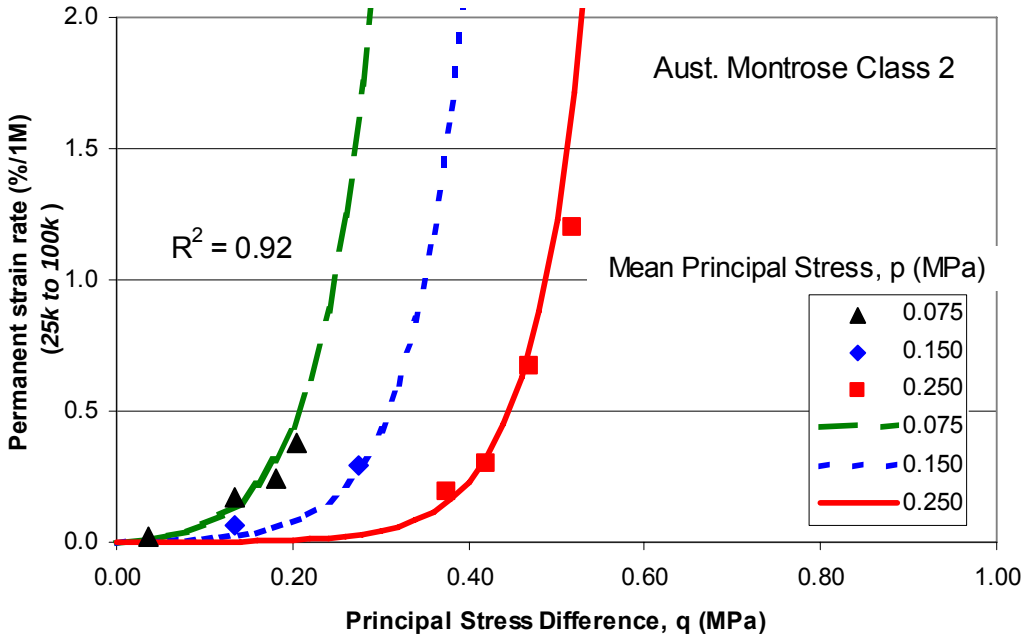

Figure 5.2 Model predictions in comparison to measured RLT data for the basecourse of Montrose Class 2 aggregate.

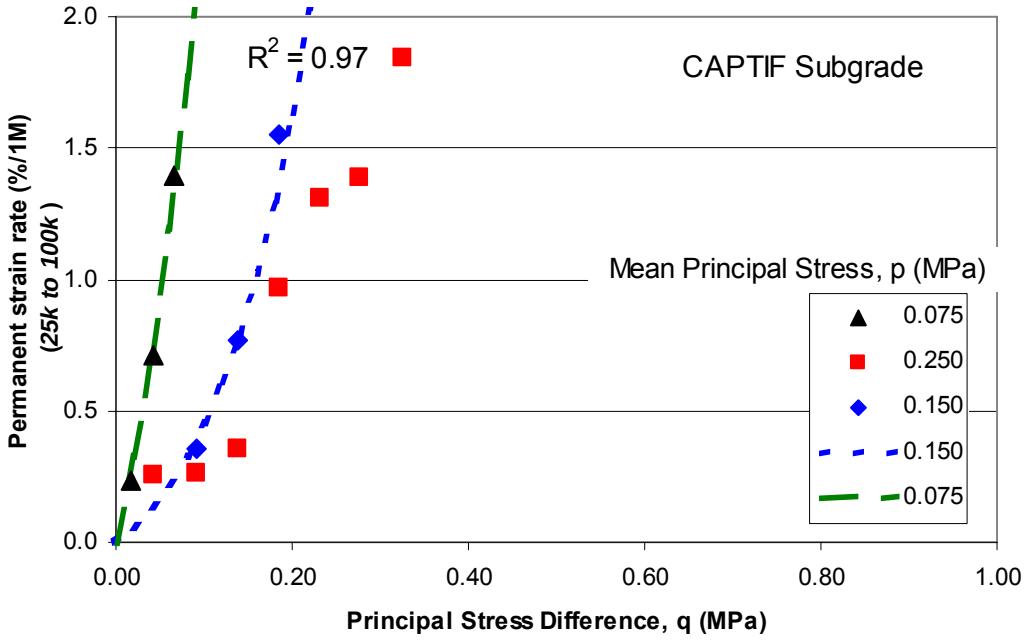

Figure 5.3 Model predictions in comparison to measured RLT data for the CAPTIF subgrade.

$$\varepsilon_{pN} = \varepsilon_{pC} + \varepsilon_{p25k\_100k} + \varepsilon_{p100k\_N} \quad \text{Equation 5.4}$$

$$\varepsilon_{pC} = C\,\varepsilon_{rate(100k\text{-}1M)} \quad \text{Equation 5.5}$$

$$\varepsilon_{p25k\_100k} = \varepsilon_{rate(25k\text{-}100k)}\,(0.75) \quad \text{Equation 5.6}$$

$$\varepsilon_{p100k\_N} = \varepsilon_{rate(100k\text{-}1M)}\,(N\text{-}0.1) \quad \text{Equation 5.7}$$

where:

- ε_{pN} = total permanent strain in % for N wheel loads (N>100,000)
- ε_{pC} = permanent strain that occurs in the first 25,000 wheel loads
- ε_{p25k_100k} = permanent strain that occurs from 25,000 to 100,000 wheel loads
- ε_{p100k_N} = permanent strain that occurs from 100,000 to N wheel loads
- N = number of wheel loads in units of millions
- C = compaction component factor to account for deformation in the first 25,000 wheel loads (value used was 0.25)
- $\varepsilon_{rate(25k\text{-}100k)}$ = permanent strain rate in % per 1,000,000 loads from 25,000 to 100,000 loads
- $\varepsilon_{rate(100k\text{-}1M)}$ = permanent strain rate in % per 1,000,000 loads from 100,000 to 1,000,000 loads

Prediction of the permanent strain rate (Equation 5.3) and ultimately permanent strain (Equation 5.4) requires inputs of stress invariants p and q. Therefore, to predict the total permanent deformation of a pavement, the stress invariants at increments of depth below the load are required. Total permanent strain calculated at each depth increment is multiplied by the associated layer thickness to compute the deformation. These deformations are added together to determine the vertical surface deformation (VSD). Linear elastic analysis of the pavement using CIRCLY (Wardle 1977) is one method to compute the principal stresses at depth increments. However, this method does not take into consideration the non-linear stiffness characteristics of the pavement aggregate and subgrade materials. The finite element program DEFPAV, that takes into account non-linearity of material stiffness, developed in 1976 at Queens University Belfast and Trinity College Dublin was used to compute stresses within the pavement.

5.4 Pavement model validation

DEFPAV was used to compute principal stresses at various depth increments for the Cptf_A03 pavement. Inputs to define the material's stiffness with different levels of stress were changed in a manual iterative procedure until the computed strains and surface deflections matched as close as possible to those that were measured. These computed principal stresses were used in a spreadsheet to calculate mean principal stress p, and principal stress difference q. Vertical surface deformation (VSD) at 25,000, 50,000, 100,000 and 1,000,000 wheel passes was then calculated using the model described in Section 5.3 for both 40 kN and 60 kN half-axle loads with a tyre contact stress of 550 kPa. This loading was the same that actually occurred in the CAPTIF pavement test.

The predicted VSD and pavement life calculated by extrapolating the results using a linear method are shown in Table 5.3. Table 5.3 also shows the associated damage law exponent calculated from the predicted lives along with actual measured values. As can be seen, the predictions of VSD at 1,000,000 wheel passes are higher than those that actually occurred but the resulting damage law exponents are close to the measured values. A beneficial residual horizontal stress of 15 kPa was added to the aggregate layers to calibrate the model in terms of damage law exponent. The compaction factor *C* (Equation 5.5) could be lowered to reduce the predicted deformation. However, it was decided not to interfere with the model as its purpose was to determine relative differences in terms of the damage law exponent.

Table 5.3 Comparisons of predicted VSD, pavement lives and damage law exponent to those obtained from VSD measurements for Segment Cptf_A03.

Model component	VSD (mm) at 1,000,000 passes		Pavement life as passes (10^6) to VSD=15 mm		Damage law exponent
Loading	40kN	60kN	40kN	60kN	*n*
Predicted	7.8	12.6	2.3	1.3	**1.5**
Measured:					
Average:	6.1	9.6	2.9	1.7	
90% ile:	7.1	11.6	3.4	2.0	
10% ile:	5.4	8.0	2.4	1.3	**1.5**

Comparison of predicted vertical surface deformations with those measured for the first five stations in Segment Cptf_A03 are shown in Figure 5.4. As can be seen the fit of predicted to measured results is fairly close for some stations. Further, the relative difference between the two loads is close to the measured values.

5.5 Pavement model predictions

Overall the model predicts fairly well the relative differences of the 40 kN and 60 kN loads in terms of damage law exponent for the Cptf_A03 pavement. The same inputs of this model were therefore used to predict the relative differences of the two loads for other pavement types that were not tested at CAPTIF. These other pavements are:

1. A 300-mm thick pavement (i.e. same thickness as Cptf_A03) with a weak subgrade of CBR=5%;
2. A 700-mm thick pavement with a CAPTIF subgrade (CBR=10%);
3. A 700-mm thick pavement with a weak subgrade of CBR=5%.

Results of the calculated VSD for the three pavement types listed, compared to the original validated model for the Cptf_A03 pavement, are shown in Figures 5.5 and 5.6.

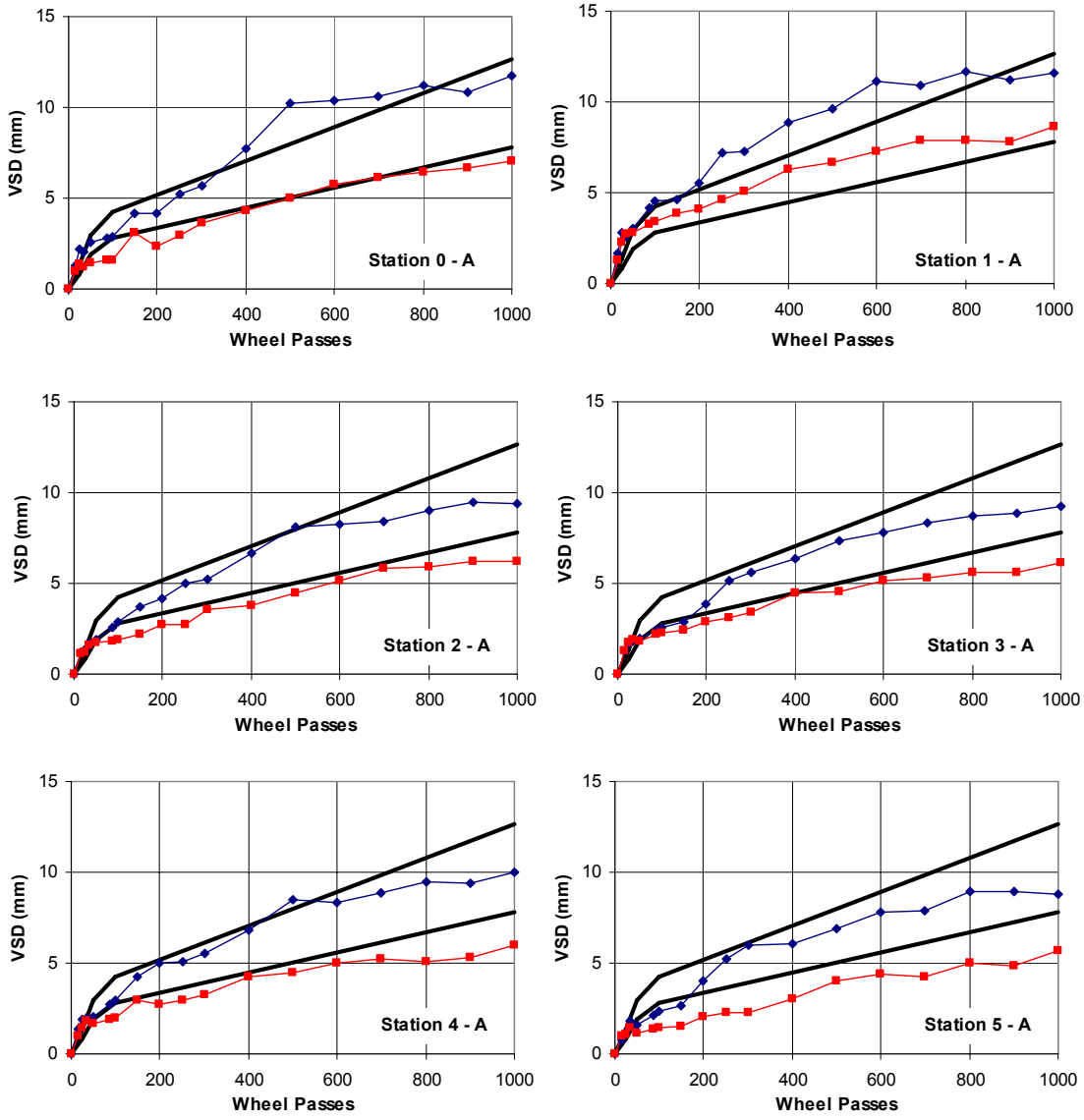

Figure 5.4 Comparison of predicted to measured VSD values for segment Cptf_A03.

Key:

▪-▪-▪-▪ 40kN measured;

♦-♦-♦ 60kN measured;

——— model (solid black line)

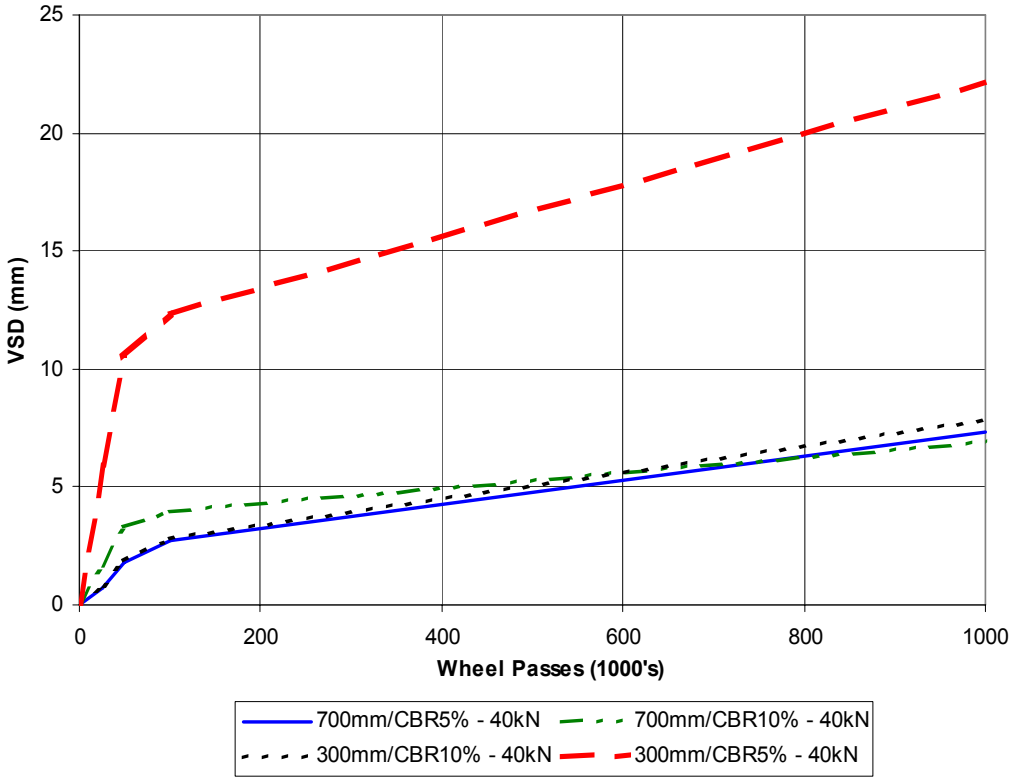

Figure 5.5 Predictions of vertical surface deformation under a 40 kN wheel load.

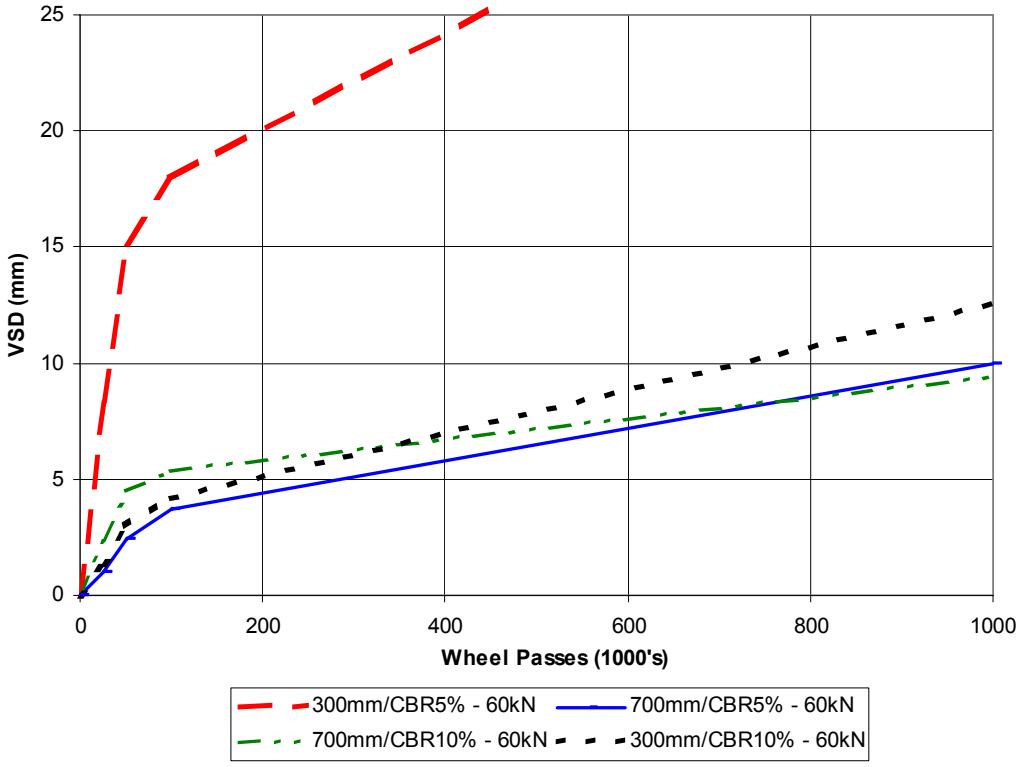

Figure 5.6 Predictions of vertical surface deformation under a 60 kN wheel load.

From the predicted VSD values, pavement lives in terms of number of wheel passes to reach a VSD of 15 mm using a linear extrapolation method, were determined. These pavement lives were used to calculate the damage law exponents detailed in Table 5.4. As was found with the analysis from the actual CAPTIF tests, there is a general trend of increasing damage law exponent with decreasing pavement strength.

To quantify the effect of pavement strength the SNP was calculated for the pavements that were modelled. Pavement layer stiffnesses, and their thicknesses that were used in the model, were used to calculate the SNP using the Ioannides (1991) method described in HTC (1999) and detailed in Equation 4.4. However, the SNP calculated from the modelled Cptf_A03 pavement was less than that found from the 10^{th} percentile value. A reason for the difference is that the modelled pavement consisted of eight pavement layers each with different stiffnesses, while the SNPs determined from the measured FWD readings were from a pavement with only two layers. Therefore, all the SNPs calculated were multiplied by 1.3 to align the SNP for the modelled Cptf_A03 pavement. This allowed the comparison of relative trends of damage law exponent as shown in Figure 5.7.

Table 5.4 Comparison of predicted pavement lives and damage law exponents for various pavement types modelled.

Pavement Type	Layer moduli	VSD (mm) at 1,000,000 passes		Pavement life as passes (10^6) to VSD=15 mm		Damage law exponent
	SNP	40kN	60kN	40kN	60kN	*n*
300 mm/CBR10%	3.5	7.8	12.6	2.3	1.3	1.5
300 mm/CBR5%	2.8	22.2	36.6	0.34	0.05	4.8
700 mm/CBR10%	4.9	6.9	9.4	3.5	2.2	1.1
700 mm/CBR5%	4.3	7.3	10.0	2.5	1.7	0.9

The limited modelling undertaken shows similar trends to the measured data where, as the SNP increases, the damage law exponent decreases (Figure 5.7). Relationships shown in Figure 5.7 are only valid for SNPs calculated from pavement layer moduli as described in Section 4.4.2 or from CBR values which may be used when designing new thin-surfaced unbound granular pavements.

Another method for calculating SNP is using FWD deflections directly as in Equation 4.9. This method has the advantage of reducing errors that could occur in the back-analysis of FWD measurements used to determine the pavement layer moduli. SNPs calculated from Equation 4.9 are less than those determined from pavement layer moduli (Equation 4.5). This is because the pavements at CAPTIF and possibly in New Zealand roads have typically high deflections while being quite strong in terms of pavement thickness and subgrade CBR.

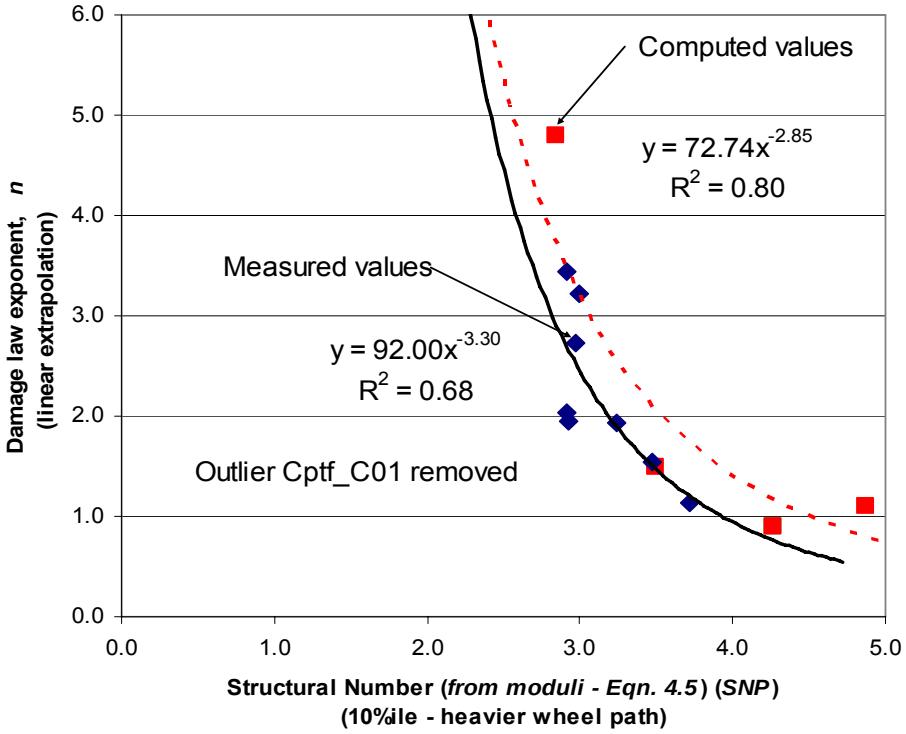

Figure 5.7 Damage law exponent (*n*) in relation to pavement structural number (SNP from pavement layer moduli) for both measured and modelled pavements.

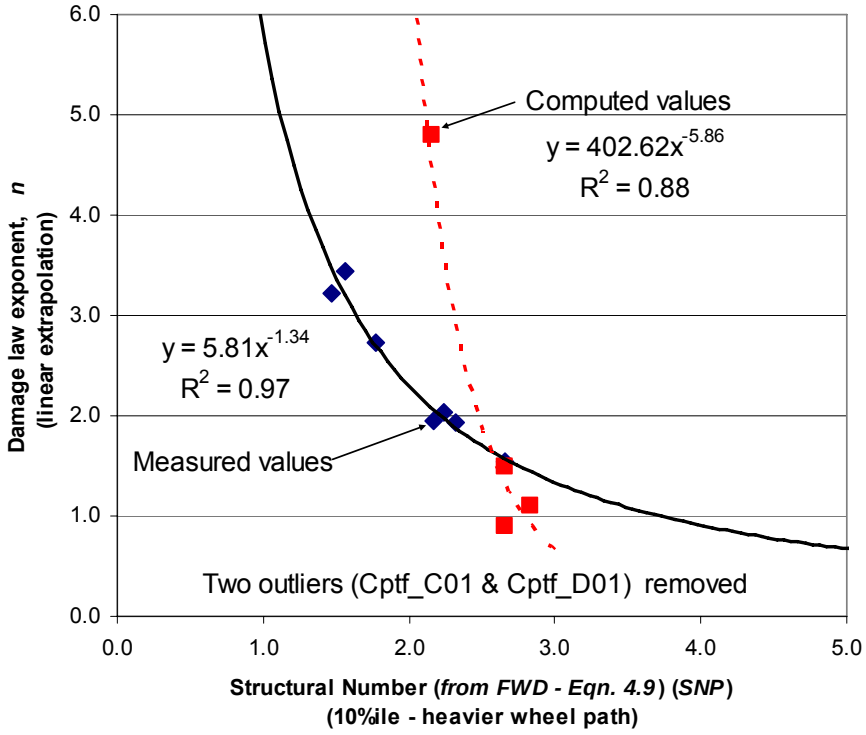

Figure 5.8 Damage law exponent (*n*) in relation to pavement structural number (SNP from FWD measurements) for both measured and modelled pavements.

DEFPAV was also used to compute the surface deflections that may have occurred from an FWD test. These deflections were used in Equation 4.9 to compute the SNP for the pavements modelled which were plotted against their damage law exponent (Figure 5.8). These calculated SNPs were multiplied by 0.88 to calibrate the SNP for the modelled Cptf_A03 pavement to the value determined from measurements. The modelled pavements did not show the same relationship of structural number to damage law exponent as did the actual measured values for pavements tested at CAPTIF. One possible reason may be an inaccuracy in DEFPAV to predict the true FWD deflections that may have occurred.

5.6 Summary

This chapter presents a new method of pavement analysis where the rut depth is calculated using RLT test data and stresses computed from a non-linear finite element package.

The model showed a capability of predicting the rut depth of the CAPTIF pavements with an accuracy that gives, in turn, the confidence for its use to predict rut depth for other pavements that have not been tested at CAPTIF.

Further, the damage law exponent calculated from the model predictions did support the trend in results found from the CAPTIF tests.

Therefore, the results from CAPTIF most likely can be extended to other pavement types, or at least to those with thin surfacings. However, the modelling work should be extended to other loads and pavements to confirm the result.

Further, the properties of the weak subgrade were estimated, and it is recommended to undertake RLT permanent strain tests on a weak subgrade and use these results for further modelling work. Finally, the model presented has applications in validating, or otherwise, current pavement design procedures and charts used for estimating pavement thickness.

6. Results, analysis and modelling for chipseal surfacing

6.1 Introduction

Increasing the mass limits of heavy vehicles is likely to reduce the life of New Zealand's chipseal surfacings. This reduction in life was found on a private forestry road where vehicles have been operating with axle loads nearly double the current legal limit in New Zealand (Arnold & Pidwerbesky 1994). The main concern is deterioration of the chipseal surfacing as represented by a loss of functional condition in terms of surface texture. Loss of surface texture will reduce the skid resistance and increase the risk of aquaplaning in wet conditions.

To assess the effect of the loss of texture two accelerated pavement tests on chipseal surfaces were conducted at CAPTIF comparing the relative chipseal lives between the standard 8-tonne dual-tyred single-axle load and axle loads of 10 tonnes and 12 tonnes. The results are summarised here with emphasis on how chipseal design and deterioration modelling methods should be modified to account for any proposed increases in mass limits. Full results of the two tests on chipseal surfaces are reported in de Pont et al. (2001) and Arnold et al. (2004, 2005a, b).

6.2 Results

Results of the chipseal studies were reported by plotting the progression of MPD (Mean Profile Depth) against load cycles for the two different wheel loads. The MPD for the whole circuit in each wheelpath was averaged, as clear trends could not be found at each individual station. A log model of the same form as the Transit New Zealand model for texture depth (Equation 6.1), developed by Patrick et al. (1998), was fitted to the measured mean profile depths (Figures 6.1 and 6.2).

$$TD = k - ALD \cdot B \cdot \log T \qquad \text{Equation 6.1}$$

where:

TD	=	texture depth
k	=	a constant which depends on ALD and bitumen spray rate
ALD	=	average least dimension of the sealing chip
B	=	a constant
T	=	total traffic to date in equivalent light vehicles (elv), where one heavy vehicle is equivalent to 10 light vehicles

Equation 6.1 for the purpose of this study was adapted to the following form:

$$MPD = k_1 - k_2 \cdot \log (N) \qquad \text{Equation 6.2}$$

where:

MPD	=	Mean Profile Depth (mm)
k_1 and k_2	=	constants
N	=	number of wheel passes

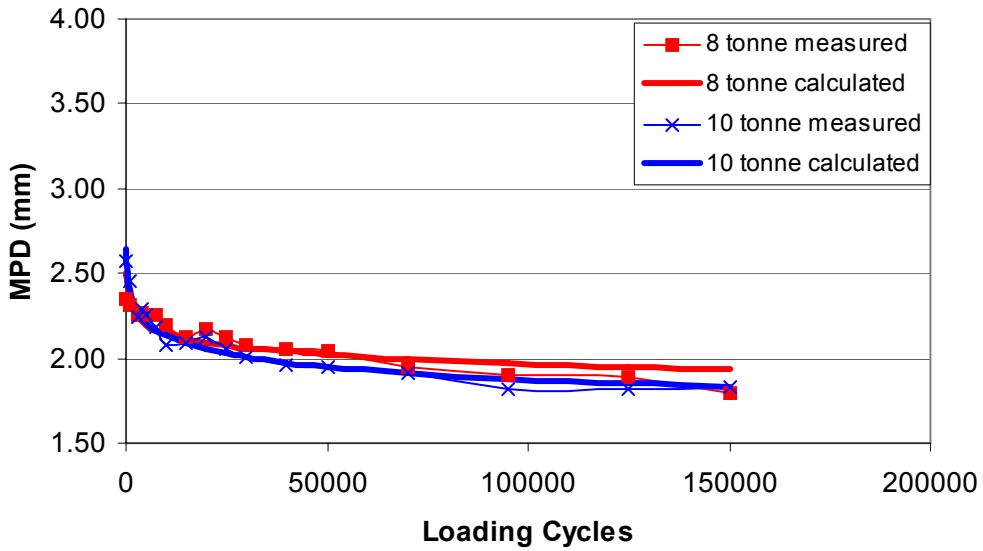

Figure 6.1 Relationship of Mean Profile Depth (MPD mm) versus loading cycles for 10 tonne and 8 tonne axle loads with Patrick log model fitted.

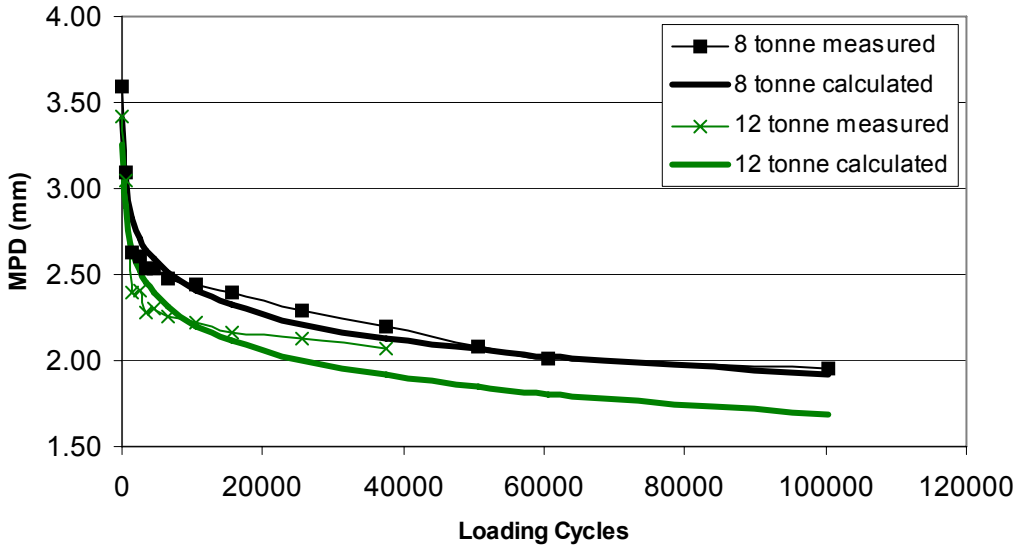

Figure 6.2 Relationship of Mean Profile Depth (MPD mm) versus loading cycles for 12 tonne and 8 tonne axle loads with Patrick log model fitted.

The constants k_1 and k_2 in Equation 6.2 were those that provided the best fit to each measured MPD curve and the resulting calculated curves are plotted in Figures 6.1 and 6.2. Table 6.1 lists the constants determined for the two tests, in which the model is seen to fit the data well, with R^2 values in excess of 0.81.

Table 6.1 Best fit constants for simplified Patrick model (for all data) using Equation 6.2.

Wheel load	Constants (Equation 6.2)		R^2
	k_1	k_2	
8 tonne *(in 8 v 10 tonnes)*	2.856	0.178	0.81
10 tonne *(in 8 v 10 tonnes)*	3.164	0.258	0.96
8 tonne *(in 8 v 12 tonnes)*	4.397	0.495	0.95
12 tonne *(in 8 v 12 tonnes)*	4.295	0.520	0.88

The Patrick model can be re-arranged to calculate the number of passes to a given MPD value, which in turn allows the determination of an appropriate damage law exponent. If the slopes (k_2) of the Patrick equation fitted to the data were identical, it would be possible to directly determine an exponent for both datasets. However this was not the case, and thus an error function was developed to determine the best fit damage law exponent. The error function was the number of ESAs using the reference load to reach a level of MPD minus the number of ESAs using the increased load to reach that same MPD. As the measurement intervals were based on a logarithmic scale, the logarithm of the error function at each interval was taken to prevent undue loading during the later stages of the testing. This error function was applied over the tests both individually and the combined datasets.

In chipseal design a key parameter is the number of light vehicle passes. It is currently assumed that 10 passes of a Heavy Commercial Vehicle (HCV) is equivalent to 10 passes of light vehicles. Based on this assumption, each pass of an 8 tonne axle is equal to α elv and each pass of a 10- or 12-tonne axle is equal to β elv. The exponents and corresponding α and β values are listed in Table 6.2.

Table 6.2 Best fit constants using the error function (provided by Equation 6.3).

Wheel load / Dataset	α	β	Damage law exponent, *n* (Equation 6.3)
8 tonne v 10 tonne	10	19	3.1
8 tonne v 12 tonne	10	23	2.0
Combined Datasets 8t v 10t	10	18	2.7
Combined Datasets 8t v 12t	10	29	2.7

6.3 Traffic volumes for chipseal design

Based on the Patrick model, one 12-tonne axle pass is estimated to be equivalent to 29 passes of light vehicles. However, the same calculation proposes that one pass of an 8-tonne axle is equivalent to 10 passes of light vehicles. By considering the relative damage of the two axle loads (8 and 12 tonnes), a damage law exponent of 2.7 is calculated.

The result that a 12-tonne axle is equivalent to 29 passes of light vehicles cannot be used directly in the design of chipseals. This is because the current method of chipseal design assumes that 1 HCV is equivalent to 10 passes of light vehicles. As an HCV is any vehicle over 4 tonnes in gross weight, a range of loads are all lumped into one type. However, should an increase in mass limits of heavy vehicles occur, then only a percentage of those HCVs will need to increase their mass limits to the new axle load limits. Therefore it is inappropriate to multiply all the HCVs by say 29 (assuming a 12-tonne axle load) to calculate the equivalent number of light vehicles.

Another method recommended for determining the number of elv for chipseal design considers the use of ESAs. Currently the assumption made in pavement design is that 1 HCV is 1 ESA (*New Zealand Supplement to the Austroads Pavement Design Guide*, Transit NZ 2000), and 1 ESA can be considered equivalent to 10 light vehicle passes for use in chipseal design.

To calculate the number of ESAs for any given traffic distribution the following equation is used as given in the Austroads Pavement Design Guide (Austroads 1992):

$$ESAs = \left[\frac{Axle\_load}{Axle\_load\_reference} \right]^{n} \qquad \text{Equation 6.3}$$

where:

ESAs = number of standard axles (Table 6.3) needed to cause the same damage as one pass of the actual axle load

Axle_load = actual axle load in kN

Axle_load_reference = reference load depending on the axle load group as defined in Table 6.3

n = damage law exponent (commonly = 4)

Table 6.3 Reference axle loads (from Table 7.1 in Austroads 1992).

Axle: Tyres:	Single Single	Single Dual	Tandem Dual	Triaxle Dual
Load (kN)	53	80	135	181

The damage law exponent *n* (Equation 6.3) is usually assumed to be equal to 4. However, for axle loads greater than those listed in Table 6.3, then the exponent used should be 2.7 as found in the 8- versus 12-tonne study of chipseal deterioration (Figure 6.3, Table 6.2). Finally, the number of ESAs (calculated for all loads) are multiplied by 10 to determine the number of elvs for the purpose of chipseal design.

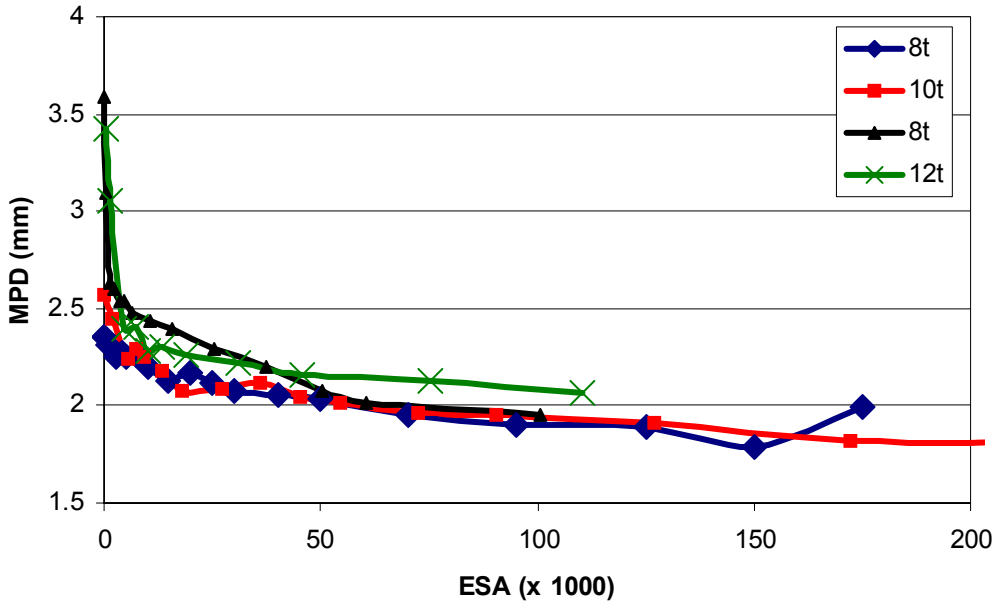

Figure 6.3 Measured MPD versus ESAs calculated with a damage law exponent of 2.7 (from Table 6.2).

7. Road User Charges

The subject of Road User Charges (RUCs) has not yet been mentioned in this report because the component of RUCs for payment of damage to the road network is covered by using the same damage law exponent *n* as that used in pavement design (see Equation 2.1).

One of the findings of this report suggests that the value of damage law exponent *n* depends on the pavement strength. Pavement strength has been classified by way of structural number (SNP) as used in dTIMS deterioration modelling. Low strength pavements (low SNPs) will result in high damage law exponents of 4 or greater, while medium and high strength pavements (medium and high SNPs) suggest an exponent of less than 4 and sometimes as low as 1 is more appropriate.

8. Conclusions

In response to possibly inevitable increases in mass limits on New Zealand roads, a four-year research study (2000-2004) was undertaken at Transit New Zealand's pavement testing facility, CAPTIF. This report analyses the accelerated pavement test results together with results from pavement analyses with the aim of modifying procedures in pavement design and deterioration modelling to account for increases in mass limits. Road User Charges (RUCs) are governed by other pressures and are not discussed in detail but, in general, the results of this study in terms of assigning the appropriate damage law exponent for pavement design would also be appropriate for RUCs.

General

- VSD, which is a fundamental form of pavement wear that results in both rutting and increased surface roughness, again proved to be the most useful measure for monitoring pavement wear at CAPTIF.
- The end-of-life for the pavement segment was defined as the number of wheel passes when 10% of the area has a VSD greater or equal to 15 mm.
- Only a small range of pavements was tested at CAPTIF. The subgrade used at CAPTIF for all pavement test segments was a silty clay with a CBR of 11%, while the aggregate types were different, and the pavement thickness was either 300 mm or 250 mm.
- The damage law exponent that relates the relative lives of axle loadings to a standard load is a key parameter used in calculating RUCs. It is also used to determine the design traffic loading in terms of ESAs for pavement design and deterioration modelling. Therefore assessing the impact of increases in mass limits by way of determining the appropriate damage law exponent has the advantage of being able to input the results of this research directly into calculating RUCs, pavement design and deterioration modelling.
- The results and analysis of the previous CAPTIF mass limits are covered more fully in other reports (de Pont et al. 2001, 2002; Arnold et al. 2001, 2003, 2005a,b).

Pavement Life

- Pavement life, in terms of the number of wheel passes until the VSD was equal to 15 mm, was best estimated by a best fit linear projection to the data from 150,000 to 1,000,000 cycles (after the initial compaction period).
- This linear projection is effectively the compaction–wear model proposed in previous reports for the mass limits study (VSD = Comp. + N **.** Wear).
- An extrapolation power model was also fitted to the data to determine the pavement life, but its use was rejected because it predicts unrealistic pavement lives. Further, the World Bank HDM-III deterioration models also assume a linear model for rut depth and thus the linear projection was adopted.

- The end-of-life for the pavement segment was defined as the number of wheel passes when 10% of the area had a VSD greater than or equal to 15 mm. This was calculated as the 10^{th} percentile value of lives for each individual station in each segment and wheelpath.
- With the exception of the segments of the 2003 CAPTIF pavement constructed with rounded aggregates (Cptf_E03), the 2001 pavement using the Australian aggregate (Cpft_C01), and the 2001 pavement constructed with recycled crushed concrete, nearly all pavements had lives between 2,400,000 and 2,800,000 passes of the 40 kN dual-tyred wheel load (which is equivalent to the current legal load of a single dual-tyred axle of 8.2 tonnes).
- The Cptf_E03 pavement had a life of 400,000 passes of a 40 kN dual-tyred wheel load.
- The Cptf_C01 pavement had a life of 4,500,000 passes of a 40 kN wheel load. However the results from this pavement were omitted because it had required many surface repairs. These had the effect of reducing the measured VSD.
- The Cptf_D01 pavement constructed with recycled crushed concrete was the best performer, as it achieved a predicted pavement life of 4,300,000 passes of a 40 kN dual-tyred wheel load. This is almost twice the life achieved with the other pavements of the same depth.

Pavement Damage Law Exponents, n

- Based on the pavement segment lives predicted in the heavy (50 or 60 kN) and light (40 kN) wheelpaths, the calculated damage law exponents ranged from 1.1 to 3.4.
- The lowest damage law exponent of 1.1 was calculated for the Cptf_D01 pavement constructed with recycled crushed concrete.
- A damage law exponent of 3.2 was calculated for the pavement constructed with rounded aggregate which had the shortest life (Cptf_E03). This suggests that the damage law exponent is related to pavement strength.

Subgrade Strain

The use of back-calculated vertical compressive strain on the top of the subgrade, as used in pavement design to predict life, was tested on the results of the CAPTIF pavement segments. FWD measurements at 50,000 wheel passes were back-analysed to determine pavement layer moduli which, in turn, were used to calculate subgrade strain. Results of this analysis were:

- For CAPTIF segments with nearly the same pavement life (approximately 1,200,000 passes of a 12-tonne dual-tyred axle), the subgrade strain calculated ranged from 1500 to 2500 micro-strain. This equates to a range of lives predicted with the Austroads subgrade strain criterion of between 6,000 and 240,000 cycles.
- The Austroads subgrade strain criterion grossly underpredicts the pavement life between 5 and 200 times less than the actual life.
- Subgrade strain varied significantly and bore no relationship to pavement life.

Pavement Structural Number (SNP)

SNP is a single parameter that classifies pavement strength and has been widely used in deterioration modelling (dTIMS, HDM) and in AASHTO pavement design. Two methods of calculating the SNP, as recommended by Transit New Zealand, were investigated for relationships between pavement life and/or damage law exponent.

The first method used to calculate SNP relied on the pavement layer moduli back-calculated from FWD measurements (referred to as 'SNP – from moduli – Equation 4.5'), while the second method used the FWD measurements directly in an equation (referred to as 'SNP from FWD – Equation 4.9').

Results of this analysis were as follows:

- Relationships between SNP and pavement life are best when using the 10^{th} percentile value of SNP and, unless otherwise mentioned, this is the value that is used in this report.
- Relationships between SNP and pavement life are best in the heavier (50 kN or 60 kN) wheelpaths.
- The Cptf_E03 segment constructed with rounded aggregate that had the shortest life was not identified as having a low SNP when calculated from pavement layer moduli. However the lowest SNP was calculated for this segment using the FWD measurements directly in the 'SNP from FWD' equation.
- Excluding Cptf_E03, the 'SNP value from moduli' compared with SNP from FWD showed the best relationships with pavement life (R^2= 0.65 in the heavier wheelpath and R^2=0.36 in the lighter wheelpath).
- Good relationships between 'SNP from moduli' and damage law exponent were obtained if the results for the Cptf_C01 segment were omitted. (Cptf_C01 had had surfacing repairs, so its removal was justified.)
- Good relationships between 'SNP from FWD' and damage law exponent were obtained if the results for Cptf_C01 and Cptf_D01 segments were omitted. (Cptf_C01 had had surfacing repairs and thus its removal was justified, while Cptf_D01 was constructed with recycled crushed concrete which has a cementing action that could affect the results.)
- The relationship with SNP determined from pavement layer moduli is best to use for the design of new pavements, while the relationship from FWD measurements is best used when interpreting FWD measurements on existing pavements.
- The best relationships found between the two different methods of calculating SNP and damage law exponent for the CAPTIF pavements tested are shown in Figure 8.1:

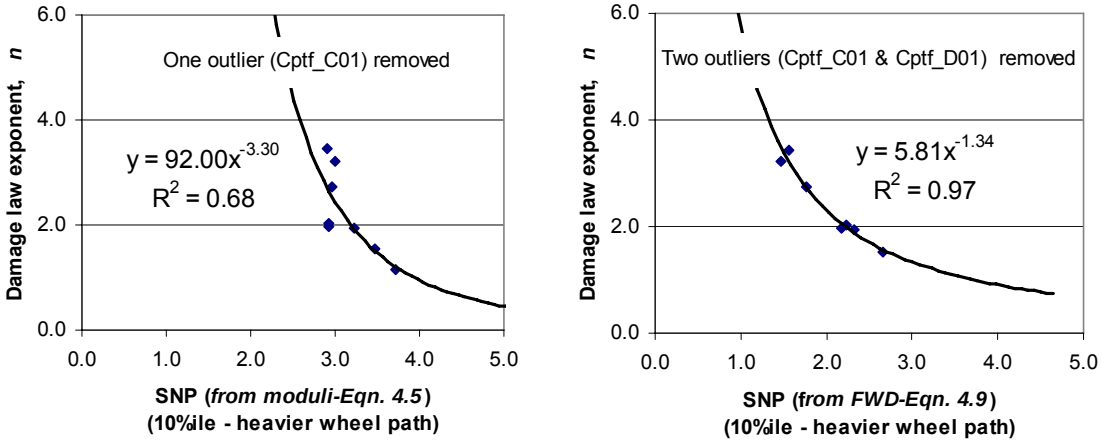

Figure 8.1 Relationships between SNP and damage law exponent *n* from CAPTIF tests.

- FWD measurements are best for predicting weaknesses in pavements that have been trafficked.
- Reasonable relationships using the damage law exponent could only be determined from FWD measurements made in the heavy wheelpath after at least 30,000 wheel passes. This suggests that FWD surveys carried out before the introduction of any increase in mass limits may not identify areas of pavement weaknesses where a high damage law exponent is considered the most appropriate.

Initial Deformation

- Without exception for all new pavements, a significant amount of deformation occurs in the first 150,000 cycles.
- This initial deformation can be predicted adequately using the HDM-III method for calculating the secondary compaction rut depth, because the damage law exponent for the compaction portion is the same as that determined from the pavement lives. Therefore the ESAs calculated in the formula for rut depth caused by secondary compaction are correct.
- With the exception of three pavement segments, increasing load on the wheelpath previously trafficked with 1,000,000 passes of the 40 kN wheel load resulted in additional secondary compaction similar in magnitude to that which occurred on the newly constructed pavement for the same load.
- Two of the three pavements that did not suffer secondary compaction caused by an increase in load on an already trafficked pavement, had been constructed with the Australian aggregate from Montrose, Victoria.
- The other pavement that did not undergo secondary compaction because of an increase in load on an already trafficked pavement, had been constructed using New Zealand AP40 aggregate complying with TNZ M/4 but contaminated with 10% by mass of silty clay fines.

Pavement Modelling

The range of CAPTIF pavements studied was limited in size. Thus to determine if trends in results could be applied to other pavement depths and subgrade strengths, additional pavements were modelled. Pavement modelling involved the utilisation of permanent Repeated Load Triaxial (RLT) data at a range of stresses along with a finite element model to compute pavement stresses. For each computed pavement stress a permanent strain value interpreted from the RLT tests was assigned. The permanent strains were multiplied by an appropriate layer thickness and summed to determine the vertical surface deformation (VSD). Results from the pavement modelling undertaken are as follows:

- The predicted VSD from the pavement model was slightly higher than the measured values for the CAPTIF pavement used for validation.
- The relative differences between the 40 kN and 60 kN wear, and thus the damage law exponents that were computed with the model were the same as the actual damage law exponent determined for the test pavement.
- The model was expanded to predict the damage law exponent for thick (700 mm) and thin (300 mm) pavements over strong (CBR=10%) and weak (CBR=5%) subgrades. The results in relation to SNP are plotted in Figure 8.2:

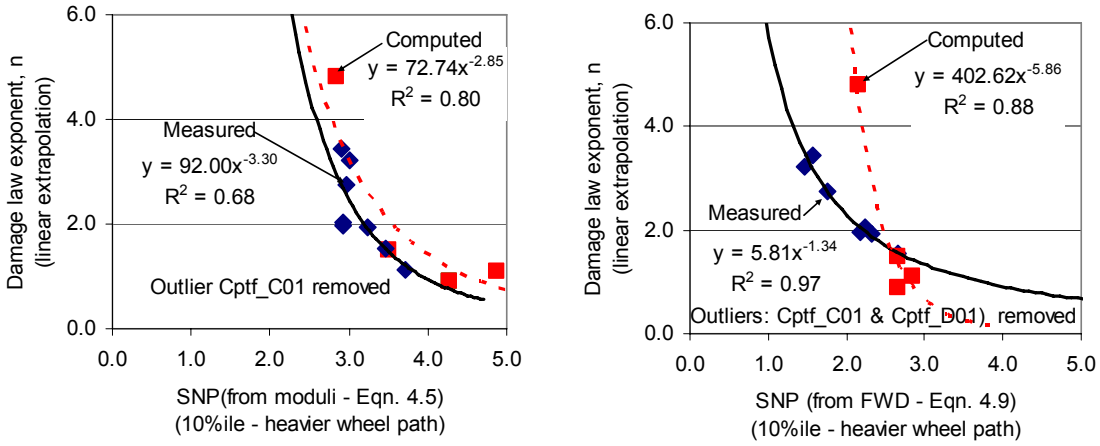

Figure 8.2 Relationships between SNP and damage law exponent *n* from CAPTIF tests (Measured) and pavement modelling (Computed). (Key: ♦ measured; ■ computed SNP values)

- The damage law exponent values computed from the pavement models supports the trends determined from the measured data. The poorer fit with the SNP determined from FWD measurements is most likely related to the inaccurate prediction of FWD deflections by the finite element program DEFPAV.
- The pavement model presented in this report represents a more fundamental method of design in terms of predicting the pavement rut depth. It can provide a method to predict the pavement life of pavements constructed with materials that do not comply with existing specifications (e.g. recycled materials). It also has application in determining damage law exponents for a range of other loads and tyre types.

Chipseal surfacing

Two tests on chipseal surfacings were conducted for 8- versus 10-tonnes and 8- versus 12-tonnes. Conclusions from these tests are as follows:

- An increase in mass limits is likely to reduce the life of chipseal surfacings on New Zealand roads. This reduction was found on a private forestry road used by vehicles with axle loads nearly double the current legal limit in New Zealand.
- The Patrick model, which forms the current basis of chipseal performance prediction, relates texture depth with the number of passes of light vehicles. It also fits well the mid-range of the measured mean profile depth (i.e. similar to texture depth) with load cycles.
- The assumption is that an 8-tonne standard axle is equivalent to 10 passes of light vehicles (i.e. in chipseal design passes of light vehicles are used, and one pass of an HCV is assumed to be equivalent to 10 passes of light vehicles). Then from the 8- versus 10-tonne test, the 10-tonne axle is equivalent to 18 passes of light vehicles, and for the 8- versus 12-tonne test the 12-tonne axle was found to be equivalent to 29 passes of light vehicles.
- Relative damage in terms of deterioration of chipseal texture depth was compared using the damage law exponent method. This comparison showed that in the 8- versus 10-tonne test a damage law exponent of 3.1 was calculated, while a value of 2.0 was calculated in the 8- versus 12-tonne test. Combining both datasets resulted an exponent value of 2.7.
- When calculating chipseal design traffic loadings in terms of number of light vehicles, ESAs should replace HCV, so that one ESA is equal to 10 light vehicle passes. This allows for an uptake by only some HCVs of any increases in mass limits, if required.

Road User Charges

- The most appropriate damage law exponent for use in RUCs should be the same value as determined from the SNP used for pavement design.
- If mass limits are increased, the damage law exponent value may be reduced from the current value of 4 for specific routes which have relatively high strength pavements. This reduction could be incorporated when assigning RUCs for vehicles which can employ the increase in mass limits.
- For the same reasons, damage law exponents for low-strength low-volume roads could increase.

9. Recommendations

Key recommendations that arise from this study are:

- When calculating traffic loading for design and deterioration modelling, then the appropriate damage law exponent in relation to the SNP should be used.
- The use of SNP is recommended to predict pavement life rather than use subgrade strain.
- As a conservative approach, existing pavements should be treated as if they are new pavements when predicting the amount of secondary compaction that is likely to result from an increase in wheel loads.
- An ESA approach should be adopted to predict the traffic loading for the design of chipseals to account for increases in mass limits.
- For specific routes with high strength pavements, the damage law exponent used in calculating RUCs could be reduced from the current value of 4. Conversely, low strength low volume pavements should use values higher than 4 for damage law exponents.
- Further pavement modelling work should be conducted to determine appropriate damage law exponents for a greater range of tyre types, loads and pavements. In particular, RLT tests on weaker subgrade materials are required in order to develop an appropriate model for pavements with weak subgrades. If pavement tests for other projects at CAPTIF are appropriate, these models could be further validated then.

10. References

AASHO. 1962. The AASHO Road Test. *Conference Proceedings: Special Report 73.* Highway Research Board, National Academy of Sciences – National Research Council, Washington DC, USA.

Arnold, G. 2004. Investigation into aggregate shakedown and its influence on pavement performance. PhD Thesis, University of Nottingham, UK.

Arnold, G., Alabaster, D.A., Steven, B.D. 2001. Prediction of pavement performance from repeat load tri-axial tests on granular materials. *Transfund New Zealand Research Report No. 214.* 120pp.

Arnold, G., Steven, B., Alabaster, D., Fussell, A. 2005a. Effect on pavement wear of increased mass limits for heavy vehicles – Stage 3. *Land Transport New Zealand Research Report 279.* 112pp.

Arnold, G., Steven, B., Alabaster, D., Fussell, A. 2004b. Effect on pavement wear of increased mass limits for heavy vehicles – Stage 4. *Land Transport New Zealand Research Report 280.* 30pp.

Austroads. 1992. Pavement Design – A guide to the structural design of road pavements. *Austroads Publication No. AP-17/92*. Austroads, Sydney, NSW.

de Pont, J., Steven, B., Alabaster, D., Fussell, A. 2001. Effect on pavement wear of an increase in mass limits for heavy vehicles. *Transfund New Zealand Research Report No. 207.* 55pp.

de Pont, J., Steven, B., Alabaster, D., Fussell, A. 2002. Effect on pavement wear of an increase in mass limits for heavy vehicles: Stage 2. *Transfund New Zealand Research Report No. 231.* 50pp.

Houghton, L.D., Hallett, J.E. 1987. An analysis of single-coat seal design. *New Zealand Roading Symposium (1987) 2:* 249-263.

HTC. 1999. Implementation of predictive modelling for road management. Phase 1: Preliminary dTIMS System. *Final Report DT/99/F2.* HTC Infrastructure Management Ltd.

Ioannnides, A. 1991. Theoretical implications of the AASHTO 1986 Nondestructive Testing Method 2 for Pavement Evaluation. *Transportation Research Record 1307:* 211-220. Transportation Research Board, Washington DC, USA.

Koh S.L., Yeo R.E.Y., Gleeson, B. 2002. Construction report: Australian axle load equivalence test pavements. Unpublished ARRB TR Contract Report for Austroads (APRG and AMRG). ARRB Transport Research, Vermont South, Victoria.

Patrick, J.E., Alabaster, D.J., Dongol, D.M.S. 1998. Pavement density. *Transfund New Zealand Research Report 100.*

Paterson, W.D.O. 1987. The Highway Design and Maintenance Standards Model (HDM-III). *Volume III, Road Deterioration and Maintenance Effects: Models for Planning and Management*. World Bank, Washington DC.

Pidwerbesky, B.D. 1995. Accelerated dynamic loading of flexible pavements at the Canterbury accelerated pavement testing indoor facility. *Transportation Research Record 1482:* 79-86.

Pidwerbesky, B., Arnold, G., Pollard, J. 1994. Can chipseals carry even heavier loads? Proc.
New Zealand Land Transport Symposium, Wellington 9-11 August.

Roberts, J., Roper, R. 1998. The ARRB integrated project level pavement performance and life-cycle costing model for sealed granular pavements. *ARRB Research Report ARR324.* ARRB Transport Research Ltd, Melbourne, Australia.

Steyn, W.J. vdM., de Beer, M., Visser, A.J. 1997. Thin Asphalt and Double Seal Rehabilitated Lightly Cemented Pavements: Evaluation of Structural Behaviour and Life Cycle Costs. Pp. 1181-1201 in *Eighth International Conference on Asphalt Pavements,* August 10 – 14, 1997. Seattle, Washington, USA.

Transit New Zealand. 2000. New Zealand supplement to the document, Pavement Design – A guide to the structural design of road pavements. (*Austroads Publication No. AP-17/92, 1992)*.

Vuong, B., Sharp, K. 2001. Impact of new heavy vehicles on pavement wear and surfacings: Responses-to-load testing using CAPTIF. Austroads Project T&EPN004. *APRG 01/08 (LO)* October 2001.

Vuong, B., Yeo, R., Choummanivong, L. 2003. Axle Load Equivalence ALF trial: measured versus predicted performance. Unpublished ARRB TR Contract Report for Austroads (AMRG and APRG). ARRB Transport Research, Vermont South, Victoria.

Wardle, L.J. 1977. Program CIRCLY. A computer program for the analysis of multiple complex circular loads on layered anisotropic media. User's Manual. *Geomechanics Computer Program Number 2.* Division of Applied Geomechanics, Commonwealth Scientific and Industrial Research Organisation, Melbourne, Australia.

Yeo, R., Alabaster, D. 2003. Impact of new heavy vehicles on pavement wear and surfacings: summary report on findings from 2002/03. *Austroads Project T&EPN504. RC2485-3.*